COLO HEP 398

The Search for the Supersymmetric Selectron

Elizabeth Goodman
April 15, 1998

Abstract

The theory of Supersymmetry was proposed to cancel the mass divergences caused by the inclusion of the Higgs particle in the Standard Model. Supersymmetry unifies the strong nuclear, the weak and the electromagnetic forces above 10^{14} GeV. By performing simulations of an e^+e^- particle accelerator, and by using equations derived from conservation laws and relativity, one can confirm the theoretically derived masses of Supersymmetric particles. The results of these computer simulations can also be used to determine the parameters to be used in the construction of a new linear collider.

Contents

1 Introduction

During the 1970's there was a unification of the weak and electromagnetic forces and a new understanding of the strong nuclear force. This unification and new understanding was based on gauge invariant theories, like the theory of electromagnetism. This unification led to what we now call the Standard Model. In order for the Standard Model to be gauge invariant, all particles must be massless. Since in reality the masses of all particles are not zero, we must introduce a scalar (spin zero) field called the Higgs field to generate particle masses. Particle masses develop as a result of the Higgs mechanism, which is the result of a shift in the potential of the Higgs field simultaneously with a gauge transformation of the fields of all the other Standard Model particles. This is referred to as spontaneous symmetry breaking.

Masses are generated following spontaneous symmetry breaking, but the mass of the scalar (spin 0) Higgs particle, because of renormalization, becomes infinite. Since this is not physical, we must correct it. The introduction of Supersymmetric particles in the process of the Higgs mass renormalization exactly cancels these divergences [1, pp. 341–342].

In addition, the existence of Supersymmetry helps us to unify the strong and electroweak coupling constants (equivalently, the electroweak and strong forces[1]) at a very high energy (10^{14} GeV) [2, p. 4031]. The existence of these two properties of Supersymmetry makes it an intriguing theory of particle interactions. Therefore, the search for Supersymmetric particles is important in high energy physics research, and is essential to our understanding of particle physics.

2 What is Supersymmetry?

Supersymmetry is a theory in which every observed particle of spin 1/2, like leptons and quarks, has a Supersymmetric partner of spin 0 (scalar), and every observed spin 1 particle (like gauge bosons) has a Supersymmetric partner of spin 1/2. In order for the Higgs mass divergences (discussed above) to cancel, the couplings of the interactions of these new particles is the same as those of the Standard Model. If the symmetry is exact, then the masses of the Supersymmetric particles should be the same as those of their Standard Model partners. Since that has not been experimentally

[1]Both the coupling constant α and the electromagnetic force are proportional to e^2.

observed, we must infer that the symmetry is not exact and the masses of the Supersymmetric particles may be much heavier. There are other reasons, more difficult to explain, why the masses of these Supersymmetric particles must be less that one TeV. This mass region should become accessible for experimental observation in the next decade or so.

2.1 Supersymmetric Particle Naming Conventions

Supersymmetric particles are named according to the convention that boson names have an "-ino" suffix, and fermions have an "s" prefix. For example, a quark has a Supersymmetric partner called a squark. The partner of the W boson is the Wino. Supersymmetric particles are denoted with a tilde above the regular particle's symbol (leptons are ℓ, sleptons are $\widetilde{\ell}$).

There are two exceptions to the naming conventions: the Supersymmetric neutralino ($\tilde{\chi}_1^0$) and the Supersymmetric chargino ($\tilde{\chi}_1^{\pm}$). The neutralino ($\tilde{\chi}_1^0$) is a mixture of the Zino ($\widetilde{Z^0}$) and the photino ($\tilde{\gamma}$). Similarly, the chargino ($\tilde{\chi}_1^{\pm}$) is a mixture of the Wino ($\widetilde{W^{\pm}}$) and the Higgsino ($\widetilde{H^0}$).

2.2 Minimal Supersymmetric Standard Model (MSSM)

There is more than one model for Supersymmetry. In this paper I will concentrate on the Minimal Supersymmetric Standard Model (MSSM). In this model the number of parameters is minimized, and there is one superpartner for each Standard model particle. Within the MSSM, there are five Standard Model Higgs particles and five Supersymmetric Higgs partner particles: one positively electrically charged ($H^+/\widetilde{H^+}$), one negatively electrically charged ($H^-/\widetilde{H^-}$), and three neutral Higgs particles ($h^0/\widetilde{h^0}$, $H^0/\widetilde{H^0}$, $A^0/\widetilde{A^0}$).

2.2.1 R-Parity

One possible property of the MSSM, R-parity conservation, requires that Supersymmetric particles be produced in pairs, and requires that a Supersymmetric particle decays into one Supersymmetric particle and one Standard Model particle [3, p. 58]. Eventually, following the last decay, there will be a final, stable Supersymmetric particle (the Lightest Stable Supersymmetric Particle or "LSSP") which leaves the detector unnoticed, taking with it a measurable amount of energy.[2] Energy conservation requires that this particle is stable, since there is no less massive Supersymmetric particle for it to decay into. We expect this particle to be the Supersymmetric neutralino ($\tilde{\chi}_1^0$) which interacts only via the weak force, thus avoiding detection. It is the energy carried by this particle which leaves the detector unobserved that leads to a missing energy signal.

2.3 Parameter Points

Within the MSSM, five data points are being studied, the particulars of which were determined by Dr. Uriel Nauenberg and his colleagues. The five parameter points are listed in Table 1.

Table 1: Parameter Points.

	m_0	$m_{1/2}$	A_0	$\tan\beta$	$sgn(\mu)$		production
Point 1	400	200	0	2	-1		*dominantly chargino*
Point 2	100	300	0	2	-1		*dominantly selectron*
Point 3	200	100	0	2	-1		*mixed chargino/selectron/sneutrino*
Point 5	300	130	-600	2	+1		*includes top squarks*
	$m_{\tilde{g}}$	$m_{\tilde{q}}$	$m_{\tilde{\ell}_i}$	$\tan\beta$	μ	m_A	production
Point 4	900	1000	1000	10	-100	200	*heavy, pseudo-scalar and charged Higgs production is accessible. Point 4 is a non-supergravity (non-SUGRA) point.*

The parameters of the MSSM with which the relevant quantities are determined are:

- m_0, the universal scalar mass
- $m_{1/2}$, the universal gaugino mass

[2]The Supersymmetric neutralino may be responsible for the "dark matter" in the universe.

- A_0, the universal trilinear term
- $\tan\beta$, the ratio of the Higgs field vacuum expectation value
- the sign of the Supersymmetry conserving Higgsino mixing term μ.

I have done my research on Point 2, concentrating on selectron production at 500 GeV, at both 80% left and 80% right incident electron polarization.

The masses of the Supersymmetric particles derived using these parameters are shown in Table 2. It is worth pointing out that the masses of all right-handed sleptons are the same, and the masses of all left-handed sleptons are the same. The right-handed sleptons' masses are different than the left-handed sleptons' masses.

Table 2: Supersymmetric Particle Masses (GeV).

	Point 1	Point 2	Point 3	Point 4	Point 5
$\widetilde{\chi}_1^0$	86.050	128.702	44.519	77.834	57.174
$\widetilde{\chi}_2^0$	175.451	257.218	96.998	115.291	111.459
$\widetilde{\chi}_3^0$	492.790	535.721	257.063	146.844	444.800
$\widetilde{\chi}_4^0$	501.853	542.758	273.757	292.407	464.631
$\widetilde{\chi}_1^\pm$	175.366	257.200	96.384	96.056	110.104
$\widetilde{\chi}_2^\pm$	500.898	542.463	257.063	292.457	461.631
h^0	83.254	89.919	68.287	126.957	101.419
H^0	745.465	681.879	379.217	201.056	622.512
A^0	741.215	676.893	371.321	200.000	619.908
$\mathrm{H}^\pm$	744.783	680.812	378.714	214.810	623.997
$\widetilde{q}_L$	603.273	668.380	316.728	1000.000	462.488
$\widetilde{b}_L$	520.573	621.862	274.269	1000.000	380.759
$\widetilde{t}_1$	424.437	535.830	263.725	924.844	150.651
$\widetilde{q}_R$	603.237	668.380	316.728	1000.000	462.488
$\widetilde{b}_R$	595.553	653.097	312.965	1000.000	456.583
$\widetilde{t}_2$	550.603	656.470	329.466	1096.285	494.730
$\widetilde{\ell}_L^-$	425.922	238.213	215.704	1000.000	320.641
$\widetilde{\nu}_L$	421.395	230.022	206.622	1000.000	314.603
$\widetilde{\ell}_R^-$	408.796	156.952	206.543	1000.000	307.449
$\widetilde{g}$	550.616	759.035	298.401	900.000	425.521

Experimental confirmation of these masses may be possible with a particle accelerator of sufficient energy. In order to produce a particle in an accelerator, one must provide energy at least equal to the mass of the particle. The purpose of this study is to determine methods for uncovering the Supersymmetric particles from within the Standard Model background, and to calculate their masses and compare them to the values predicted by theory.

3 Why Do We Need Supersymmetry?

The motivation behind Supersymmetry is deeply immersed in field theory. The following is a very brief explanation of the problems solved by Supersymmetry.

3.1 Mass Divergences

One of the key properties of Supersymmetric theory is the cancellation of quadratic mass divergences that affect the masses of all scalar particles. In the Standard Model, the only scalar particle is the Higgs particle. The quadratic mass divergences can be described by the Feynman diagram in Figure 1.

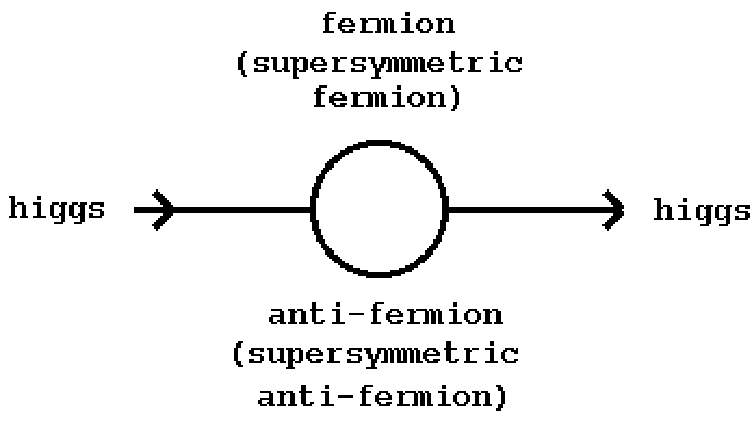

Figure 1: Feynman diagram describing quadratic mass divergences.

The calculation of the contribution of the dissociation of the Higgs field into a Standard Model fermion/anti-fermion is the quadratically divergent integral:

$$8g^2 \int \frac{d^4k}{k^2 - m^2} \tag{1}$$

This quadratically divergent integral causes the mass of the Higgs particle to be infinite.

The contribution of the dissociation of the Higgs field into a Supersymmetric fermion/anti-fermion is the quadratically divergent integral:

$$-4g^2 \int \frac{d^4k}{k^2 - m^2} - 4g^2 \int \frac{d^4k}{(k-p)^2 - m^2} + I(p,m) \tag{2}$$

where the integral I(p,m) is only logarithmically divergent. By making a change of variables in the second integral of equation (2), (k$\rightarrow$k+p), the sum of the two equations causes the two quadratically divergent terms to cancel up to I(p,m) when the coupling constants are the same [1, pp. 341-342]. The logarithmically divergent term is a problem that affects all of field theory and is easily solvable by a cut-off at extremely high energies.

3.2 Unified Forces

The renormalization of coupling constants, similarly to the renormalization of mass, make the coupling constants a function of energy. It is one of the expectations of elementary particle theory that all coupling constants will have the same value at extremely high energies. The calculation of the energy dependence based on only the presence of Standard Model particles does not meet that expectation. The introduction of Supersymmetric particles in this renormalization scheme leads to the unification of the electromagnetic, the weak and the strong nuclear coupling constants at an energy above 10^{14} GeV [2, p. 4031].

4 How Will Supersymmetry Be Observed?

Scientists search for Supersymmetric particles by colliding two normal Standard Model particles with an accelerator, and then carefully studying the particles that are observed by the detector. By measuring the initial and final momenta of the particles in the system, and by using conservation of energy and momentum, we can ascertain whether any particles escaped undetected, and the direction in which they went.

We expect to observe electrons (e^-), muons (μ^-), photons (γ), and hadrons (e.g., pions, kaons, and protons) in the detector. Electrons and photons are detected in the electromagnetic calorimeter. They cause particle showers with which we can determine the particles' energies. A magnetic coil located outside of the electromagnetic calorimeter creates a magnetic field which causes the trajectories of charged particles to bend, so one can determine their momenta, and therefore (if the particles' masses are known) their energies.

Hadrons are detected in the hadron calorimeter. Charged hadrons are observed in the tracking system. Muons are detected in the muon detector (the μ decays in 10^{-6} seconds, which is so long that it appears to be stable to the collider detector). Neutrinos always leave the detector without being detected, taking energy with them. This is because neutrinos interact only via the weak force, which is so weak that it does not interact with anything in the collider detector.

Missing energy is the signal for Supersymmetry. Missing energy can be caused by Standard Model neutrinos, Supersymmetric neutralinos and detector flaws. All detectors have some inefficiencies, and none have perfect resolution. We can minimize the detector ineffiency and try to improve the resolution, but no detector is perfect. We can identify neutrino events if we understand their production modes, and remove events that have these types of modes. The events we are left with will be Supersymmetric events (with energy missing) or identifiable non-neutrino Standard Model processes (with no missing energy).

Scientists use computer simulations to investigate the production of Supersymmetric particles in electron-positron (e^-e^+) collisions. Professor Uriel Nauenberg's high energy physics group uses existing simulation programs called ISAJET [5], PYTHIA [6], and HERWIG 5.9 [7]. We use ISAJET to generate the Supersymmetric signal and the W^+W^- background, and PYTHIA and HERWIG to generate other background modes. We program in FORTRAN on a VMS system. Our histograms are created using PAW (Physics Analysis Workstation) [8]. ISAJET and HERWIG are especially useful because they allow for both electron and positron longitudinal polarization. This longitudinal polarization helps us to understand the production of Supersymmetric particles. Our group is writing code to analyze data from electron-positron collision events. Our goal is to separate the Supersymmetric signal from the Standard Model "background" by reducing the number of background events without greatly reducing the number of signal events. We do this by programming requirements that the events being studied satisfy certain constraints. These requirements are called "cuts."

4.1 The Method Used

- perform simulations at E_{cm} of 500 GeV, where we can expect to see $e^+e^- \rightarrow \tilde{e}^+\tilde{e}^-$
- starting with 80% right polarization, separate the Supersymmetric signal from the Standard Model background by applying cuts that reduce the background without changing the endpoints of the energy histogram of the signal
- perform the same cuts on the 80% left-polarized events
- by observing which part of the histogram changes with changing polarization, we can determine where in the histogram the $\tilde{e}_R^-\tilde{e}_R^+$ events are, because their cross section changes the most with polarization
- apply a fit function to the part of the energy histogram of the E_{e^+/e^-} that changes the most with changes in polarization.
- use the endpoints of the fit (E_{min} and E_{max}) in the equations for the masses of the $\tilde{\chi}_1^0$ and the $\tilde{e}_R$.
- apply a step fit function to the whole E_{e^+/e^-} energy histogram.
- determine the mass of the $\tilde{e}_L$ by using the endpoint E_{max} of the fit to the whole E_{e^+/e^-} energy histogram, and the (now known) masses of the $\tilde{e}_R$ and $\tilde{\chi}_1^0$.

5 The Standard Model Background

The Standard Model is the theory that describes quarks and leptons and their interactions. Our "background" includes the particles that are expected to exist according to the Standard Model, in quantities that have been predicted by theorists. Table 3 lists the cross sections (in fb)[3] for our Standard Model background production modes (500 GeV).

Table 3: Cross sections (in fb) for Standard Model (500 GeV).

Mode	Cross Section	Production Fraction
$\gamma^* + \gamma^*$	4.42 x 10^7	99.6%
$\gamma + \gamma$	68400	0.154%
$\gamma^* or Z^0$	53800	0.121%
$\gamma + \gamma^* or Z^0$	52000	0.117%
$Z^0 + Z^0$	4270	0.00960%
W^+W^- (80% right polarized)	7160	0.00161%
$\gamma^* + \gamma^*$	4.42 x 10^7	99.3%
W^+W^- (80% left polarized)	113000	0.254%
$\gamma + \gamma$	68400	0.154%
$\gamma^* or Z^0$	53800	0.121%
$\gamma + \gamma^* or Z^0$	52000	0.117%
$Z^0 + Z^0$	4270	0.00957%

Our simulations do not presently include all possible background sources, but all major cross sections of background are included.

5.1 Virtual Photon Processes

Clearly, $\gamma^*\gamma^*$ dominates the background. The γ^* is a virtual particle; its intermediate state leads to the productions shown in Table 4.

The $q\bar{q}$ and $\ell\bar{\ell}$ are observed in the detector. W^+ and W^- decay as shown in Table 7.

The e^+e^- virtual photon process occurs as shown in Figure 2.

Because the initial electron and positron both usually go down the beam-hole, the visible result of this process is most often one electron and one positron.

[3]femto = 10^{-15}, barn = 10^{-24} cm^2

Table 4: Production Modes for $\gamma^*\gamma^*$.

Mode	Cross Section (fb)	Production Fraction
e^+e^-	2.76 x 10^7	62.35%
$\mu^+\mu^-$	1.24 x 10^7	28.07%
hadrons	3.93 x 10^6	8.88%
$\tau^+\tau^-$	3.09 x 10^5	0.70%
W^+W^-	111	0.02%

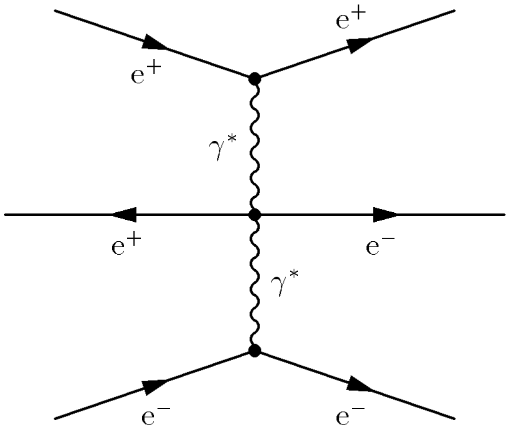

Figure 2: Feynman diagram showing the production of $\gamma^*\gamma^*$ events.

5.2 Photon Processes

The γ is massless, stable, and is detected in the calorimeter.

5.3 Z^0 Processes

The Z^0 decays as shown in Table 5. The hadrons, $e^\pm$, and $\mu^\pm$ are almost always observed, the neutrinos are unobserved, and the τ decays as shown in Table 6.

Missing energy results from the neutrinos and any particles that are unobserved due to detector inefficiency.

Table 5: Decay Modes for Z^0.

Mode	Production Fraction
hadrons	69.90%
neutrinos	20.01%
e^+e^-	3.37%
$\mu^+\mu^-$	3.37%
$\tau^+\tau^-$	3.37%

Table 6: Decay Modes for τ.

Mode	Production Fraction
hadrons + ν_τ ($\bar{\nu_\tau}$)	64.8%
e $\nu_e\nu_\tau$	17.8%
$\mu\nu_\mu\nu_\tau$	17.4%

5.4 W$^\pm$ Processes

The W particle decays as shown in Table 7. The cross section for the W^+W^-

Table 7: Decay Modes for W.

Mode	Production Fraction
2 *quarks* $\rightarrow$ *hadrons*	67.8%
$e^\pm + \nu_e(\bar{\nu_e})$	10.8%
$\mu^\pm + \nu_\mu(\bar{\nu_\mu})$	10.6%
$\tau^\pm + \nu_\tau(\bar{\nu_\tau})$	10.8%

is highly dependent on polarization because the production can occur two ways. In the first case, a ν is exchanged. Since there are no right-handed neutrinos, this process only occurs for left-handed polarizations and the cross section for left-handed W$^+$W$^-$ is much higher than the right-handed cross section. This is called a t-channel exchange.

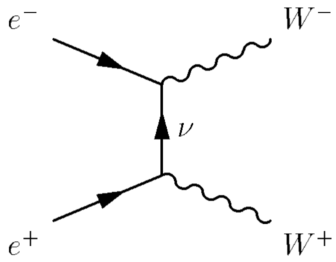

The other W boson production process involves the exchange of a Z^0 or a γ, and can occur for either left- or right-handed polarizations. This is called an s-channel exchange.

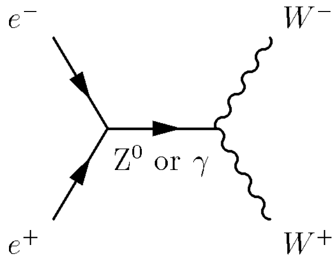

When the W decays into hadrons, little or no energy is lost and the visible energy for the event is approximately 500 GeV. When the W decays into leptons and neutrinos, the neutrinos always leave undetected. The tau is one of the leptons into which the W can decay. The tau decay modes are shown in Table 6. All $W^{\pm} \rightarrow \ell^{\pm}$ decays involve the loss of energy due to neutrinos.

5.5 Energy Histograms

It is useful to show the distribution of the energy of the visible electron or positron in each event. Most of the histograms that follow depict the energy of each visible particle in GeV vs. the number of events. All histograms depict an integrated luminosity ($\mathcal{L}$) of 50 fb^{-1}, which is the simulated equivalent of one year of accelerator run-time.[4]

[4]The integrated luminosity ($\mathcal{L}$) and the number of events observed are related by the following formulas:

$$\begin{aligned} \sigma\mathcal{L} &= \#\ \text{events/time} \\ \sigma &= \text{cross section of process} \end{aligned}$$

Integrated luminosity is the number of events per unit of time (one year in our study) divided by the cross section.

Figure 3 shows a plot of the energy of each visible electron or positron for the Standard Model background at 500 GeV for 80% right polarization. The peaks in the distribution are due to the scaling of the $\gamma^*\gamma^*$ events.[5]

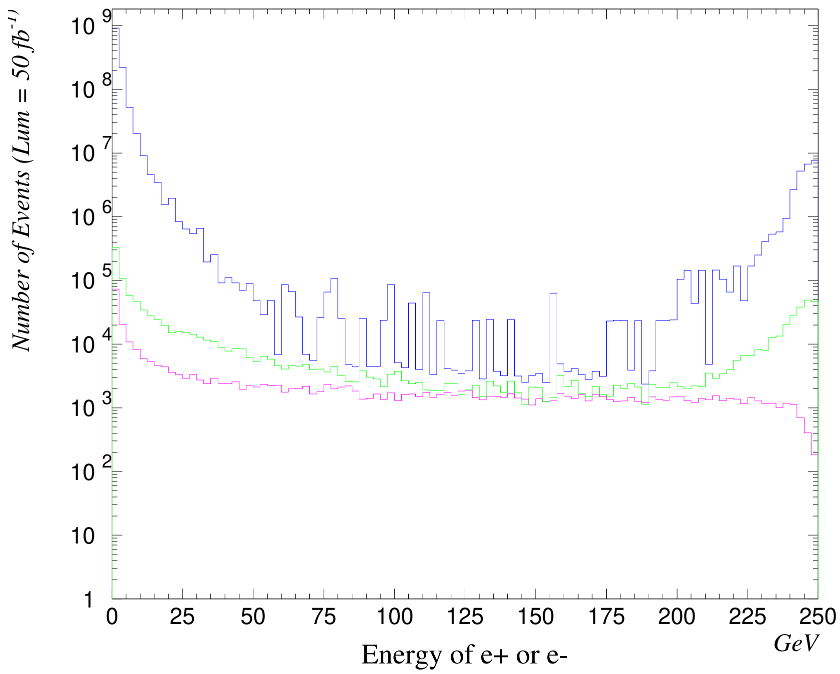

Figure 3: E_{e^+,e^-} for Standard Model background. Blue line is entire background including $\gamma^*\gamma^*$, green line is mainly Z^0 and real γ events, purple line is $W^\pm$ events. E_{cm} = 500 GeV, 80% right polarization.

The histogram in Figure 3 contains all backgrounds that we have generated. Note that the histogram is on a log scale, and the majority of events are $e^+e^- \to \gamma^*\gamma^* \to e^+e^-$.

In the $e^+e^- \to \gamma^*\gamma^* \to e^+e^-$ data, the peak at 0 GeV is due to events where both initial particles go down the beamline and are not detected leaving two visible $e^\pm$. The events around 125 GeV is where one initial particle goes down the beamline, and the 250 GeV peak is due to events where all

[5] In order to obtain 50 fb^{-1} of data, we need 1.38 x 10^9 events. Rather than generating this huge number, we began by generating 69000 $\gamma^*\gamma^*$ events and scaled each event by 20000. Following our first series of cuts, when the number of background events was substantially reduced, we generated 6.9 x 10^6 events and scaled by only 200.

four e$^{\pm}$ are visible. Tails come from the peaks because the intermediate state virtual photons have varying energies, depending on their momenta when they are generated.

The peak in the green line just under 250 GeV (half of the center of mass energy E_{cm}) is due to events with neutrinos. There are two main productions that cause this:

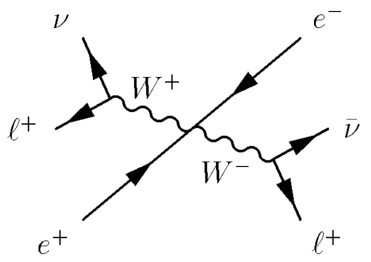

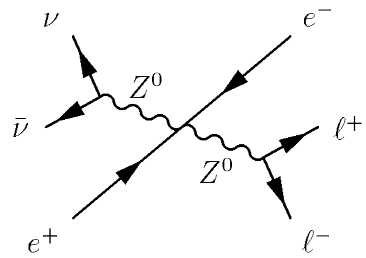

The peak from the W decays is not at exactly 250 GeV because the particles have varying momenta when they are produced, and therefore have varying energies.

6 The Supersymmetric Signal

The cross sections (in fb) for various Point 2 production modes are shown in Table 8.

Within the MSSM, we anticipate that the neutralino ($\tilde{\chi}_1^0$) is the lightest stable Supersymmetric particle. As shown in Table 2, the mass of the neutralino for Point 2 is 128.7 GeV. As a result of R-parity conservation, every Supersymmetric event has at least one neutralino. Because the neutralino interacts weakly, it leaves the detector without being detected. Although the

Table 8: Cross sections (in fb) for Point 2 production modes.

E_{cm}	350 GeV		500 GeV		750 GeV		1000 GeV	
	80% L	80% R	80% L	80% R	80% L	80% R	80% L	80% R
$\widetilde{\chi}_1^0\widetilde{\chi}_1^0$	84	294	107	360	76	246	50	161
$\widetilde{\chi}_2^0\widetilde{\chi}_2^0$					74	18	71	17
$\widetilde{\chi}_1^0\widetilde{\chi}_2^0$			56	14	75	20	60	15
$\widetilde{\chi}_1^+\widetilde{\chi}_1^-$					187	47	190	47
h^0Z^0	170	140	69	58	27	22	15	12
$\widetilde{\nu}_e\widetilde{\nu}_e$			114	31	621	163	635	165
$\widetilde{e}_L^+\widetilde{e}_L^-$			7	2	116	35	143	42
$\widetilde{e}_R^+\widetilde{e}_R^-$	20	58	85	280	91	329	78	281
$\widetilde{e}_L^\pm\widetilde{e}_R^\mp$			145	145	95	94	57	59
$\widetilde{\ell}_L^+\widetilde{\ell}_L^-$	24	52	10	4	70	31	56	26
$\widetilde{\ell}_R^+\widetilde{\ell}_R^-$			62	137	44	94	31	61
total	297	543	662	1036	1501	1124	1411	908

neutralino is the lightest stable Supersymmetric particle, its mass is clearly large enough that its effects should be easily observable because it leads to a large amount of missing energy. Therefore, none of the electrons in Supersymmetric events will have 250 GeV of energy.

6.1 Selectrons

Figure 4 shows a plot of the energy of each electron and positron for the Standard Model background (blue) and for Point 2 selectrons (red).[6] It is our goal to determine how to remove, by kinematical cuts, the Standard Model background while minimally affecting the Supersymmetric signal.

Selectrons always decay in the following manner:

[6] In Figure 4 the signals for e_Re_R, for e_Re_L, for e_Le_R, and for e_Le_L were combined to form the signal for total selectron production.

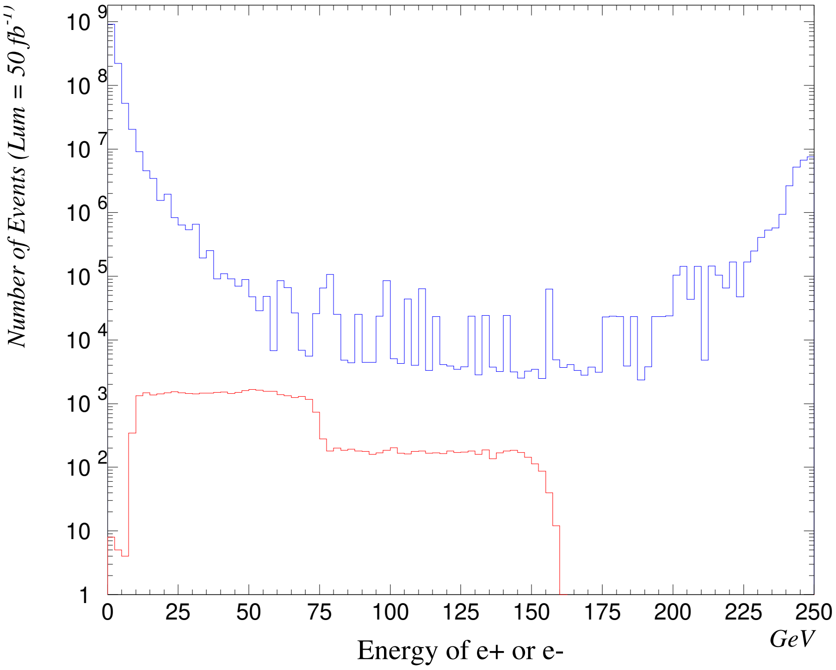

Figure 4: E_{e^+,e^-} for Supersymmetric signal (red) and Standard Model background (blue). E_{cm} = 500 GeV, 80% right polarization.

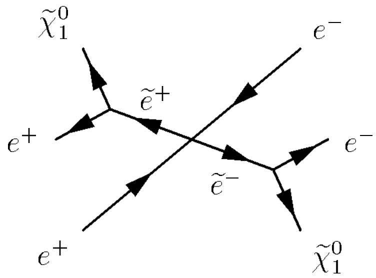

In these events, two neutralinos leave the detector unnoticed. This decay process results in a minimum of 128.7 GeV of missing energy in each visible electron due to the mass of the neutralino, with additional missing energy due to the neutralino's kinetic energy. Because the mass of the electron is so small compared to that of the neutralino, the neutralino carries the majority of the kinetic energy. Because of this, the signal for the Supersymmetric particles appears below 250 Gev.

Generally, the energy histogram of a two-body decay is square or rectangular. The shape of our Supersymmetric signal is not exactly that of a typical two-body decay. This is because our Supersymmetric signal is made of $\tilde{e}_L\tilde{e}_L$, $\tilde{e}_R\tilde{e}_L$, and $\tilde{e}_R\tilde{e}_R$ events. The cross section for each group is different. The largest cross section is for the $\tilde{e}_R\tilde{e}_R$ events, and the signal for the $\tilde{e}_R\tilde{e}_R$ is in the square on the left side of the signal. The next largest cross section is for $\tilde{e}_R\tilde{e}_L$ events, and these events occupy the majority of the rest of the signal. The cross section for the $\tilde{e}_L\tilde{e}_L$ events is very small, and the signal for them is unnoticeable next to the $\tilde{e}_R\tilde{e}_R$ and $\tilde{e}_L\tilde{e}_R$ events.

The events between 0 and about 8 GeV in the Supersymmetric signal are events where one of the two electrons is invisible because it goes down the beamline. The particle that goes down the beamhole is highly energetic, so the remaining particle has less energy and is therefore on the low end of the energy spectrum.

It is clear that in Figure 4 the number of events of the background completely obscures the Supersymmetric signal. Therefore, when evaluating data from e^+e^- collisions, it is necessary to separate Supersymmetric events from Standard Model events. To separate the signal from the background, in our computer programs we add requirements that the events being studied satisfy certain constraints. These requirements are called "cuts," because they effectively cut out unwanted events. In our research, we want to enhance the signal from Supersymmetric events by reducing the background, so we include cuts that remove Standard Model background without affecting the endpoints of the Supersymmetric signal. In order to accurately simulate the capabilities of an actual detector, the cuts we make are those that can be duplicated by the detectors in a real e^+e^- collider. It is important to maintain the edges and the shape of the signal in order to correctly calculate the masses of the supersymmetric particles as shown in the appendices. As we apply the cuts, we need to ensure that the lower endpoint stays at 7.5 GeV and the upper endpoint stays at 160. It is also important to maintain the shape of the histogram because after applying cuts we apply a gaussian fit function to our distribution. If the shape of the distribution has changed, the endpoints of the gaussian will change.

6.1.1 500 GeV, 80% right polarization

Since the largest visible production mode is $\tilde{e}_R^+\tilde{e}_R^-$ at 500 GeV, 80% right polarization, we begin by studying this process. The Supersymmetric signal includes $\tilde{e}_R^\pm\tilde{e}_R^\mp$, $\tilde{e}_R^\pm\tilde{e}_L^\mp$, $\tilde{e}_L^\pm\tilde{e}_R^\mp$, and $\tilde{e}_L^\pm\tilde{e}_L^\mp$.

Cut 1 Figure 5 shows the Standard Model background (blue) and Supersymmetric signal (red) at 500 GeV, 80% right polarization, after limiting the events to those with exactly two visible particles: one electron and one positron. This dramatically reduces the background. In the virtual photon events, all of the events over about 175 GeV have more than two visible particles, so these events are cut. The production of $e^{\pm}$ occurs only in 3.36% of Z^0 decays and in 10.8% of W decays. Since *both* Z^0's or *both* W's must go to $e^{\pm}$, the probability of the two events happening is the product of the probability of each event. The chance of both W particles decaying into $e^{\pm}$ is $10.8 \times 10.8 = 1.17\%$, and for the Z^0's it is .11%. All selectron events result in the production of an electron and a positron. Therefore, this cut only affects the signal when the electron or the positron goes down the beampipe. As can be seen from Figure 5, the Supersymmetric signal is now distinguishable from that of the background. In order to improve our mass measurement, we need additional cuts to observe the leading and lagging edges of the electron or positron energy distribution.

Angular Distribution In Standard Model events, the $e^+ + e^- \rightarrow W^+ + W^-$ occurs either with the exchange of a Z^0 or γ particle or with the exchange of a ν. In the first case, the cross section is approximately proportional to $1 + \cos^2(\theta)$ (θ is measured relative to the beam axis); with the exchange of a ν, the cross section is proportional to $1/\sin^4\frac{\theta}{2}$. In both cases, the resulting cross section is much bigger for θ near 0 and π. The signal events do not exchange the ν or the Z^0, and decay products are approximately uniform through all angles. Figure 6 shows the angular distribution of particles in the detector. The distribution is approximately the same for both 80% left and 80% right polarizations.

Cut 2 The second cut, Figure 7, limits the events to those that have less than 1 GeV visible energy between $.90 < |\cos(\theta)| < .995$.[7] Figure 6 shows that the e^+ or e^- from selectrons occur approximately uniformly through all angles and that background particles occur mostly along the beam axis toward $|\cos(\theta)| = 1$. By removing events with energy between $.90 < |\cos(\theta)| < .99$, we reduce the Standard Model background without much affecting the Supersymmetric signal.

[7] We use $\pm .995$ for our upper limit because energy is not visible above $|\cos(\theta)| = 0.995$

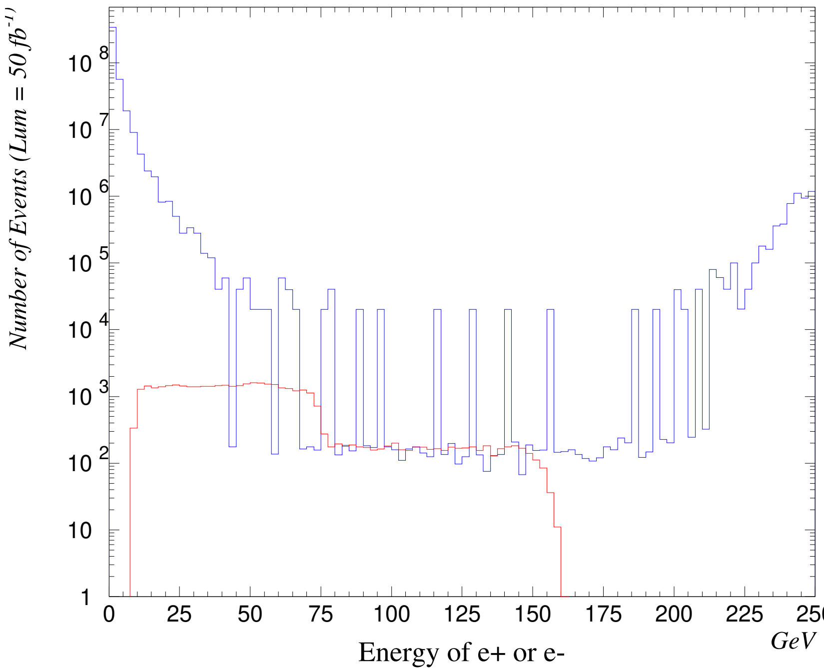

Figure 5: E_{e^+,e^-} for Supersymmetric signal (red) and Standard Model background (blue) following cut to limit events to those with exactly two visible particles: one electron and one positron. E_{cm} = 500 GeV, 80% right polarization.

Cut 3 If there were no invisible particles leaving the detector, and if the detector was perfectly efficient, the energy in the forward direction[8] should be $\sim 1/2$ E_{cm}, and the energy in the backward direction should be $\sim 1/2$ E_{cm}. Nevertheless, all Supersymmetric events have some energy missing (usually in both hemispheres), and therefore will not have $E_{forward} \sim 1/2$ E_{cm}. Figure 8 only includes events with visible energy in the forward direction less than 1/2 E_{cm} minus 10% E_{cm}.[9]

In the following type of event both the electron and the positron produced by the Z^0 are detected as long as they don't go down the beampipe. This process results in energy in the forward direction having energy $\sim 1/2$ E_{cm},

[8]The forward direction is the hemisphere around the thrust axis that has more visible energy.

[9]The 10% is subtracted to account for detector inefficiency and resolution.

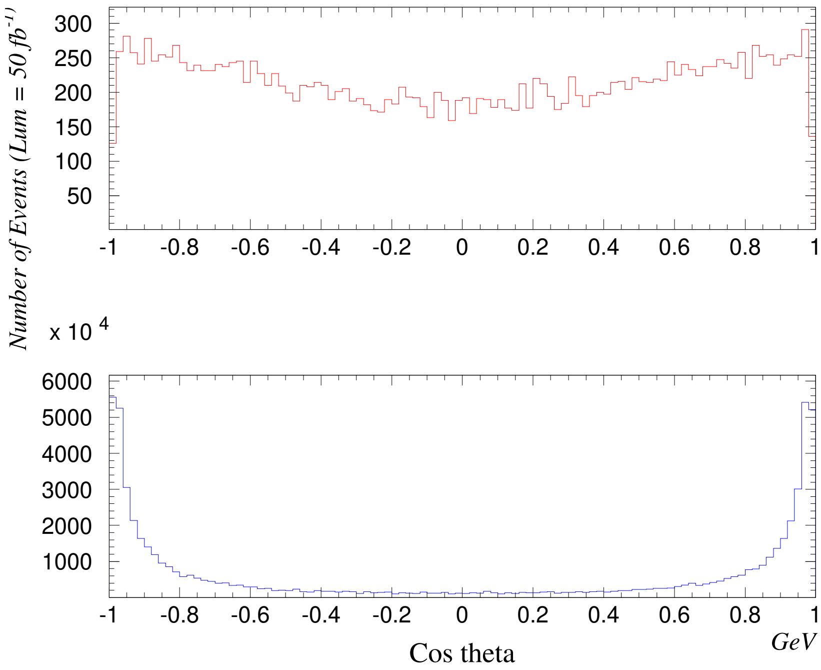

Figure 6: Cos(θ) for visible particles at 500 GeV, 80% right polarization. The spectrum for Supersymmetric particles (top, red) is approximately uniform through all angles. The spectrum for Standard Model background particles (bottom, blue) peaks at cos(θ) near $\pm$ 1. (Varying the polarization does not affect the angular distribution.)

and is therefore cut.

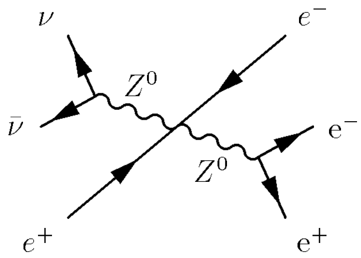

The Supersymmetric events generally produce an electron and a neutralino in one hemisphere, and a positron and a neutralino in the other hemisphere.

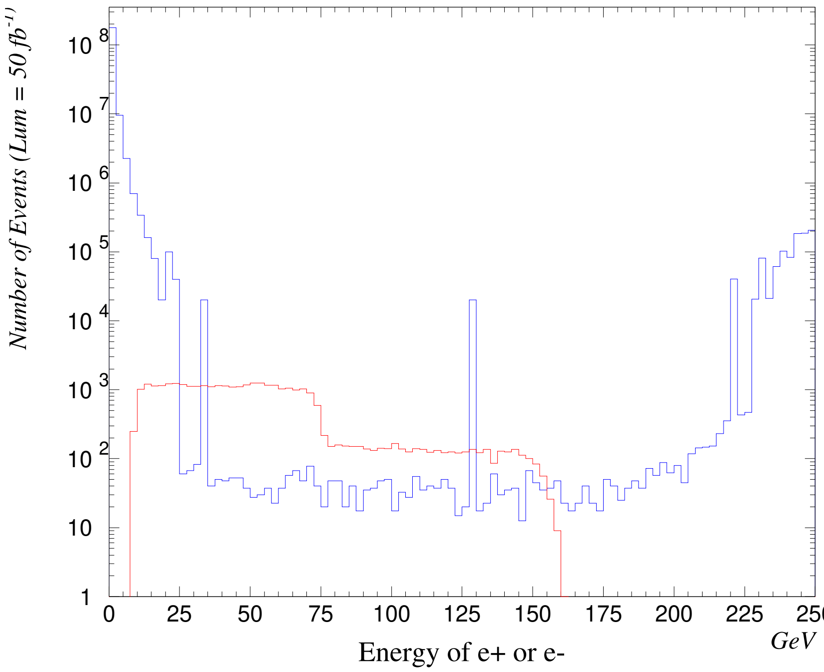

Figure 7: E_{e^+,e^-} for Supersymmetric signal and Standard Model background following cut to limit events to those with less than 1 GeV visible energy between 0.9< $|\cos(\theta)|$ <.99. E_{cm} = 500 GeV, 80% right polarization.

Neither hemisphere has energy greater than 1/2 E_{cm} minus 10% E_{cm}. Therefore, by cutting out events with energy greater than 1/2 E_{cm} minus 10% E_{cm}, we remove background without affecting the signal.

Cut 4 The proposed design for the NLC[10] incorporates a luminosity monitor. The luminosity monitor is made up of one ring at each end of the detector, with the beamline going down the center of it. It occupies the space between .995 < |Coszeta| < .99995. We can often detect the initial electron and positron (after the γ^* are emitted) in the luminosity monitor, and we find that their energies are usually more than 200 GeV. We also detect very forward e^+ or e^- from $W^\pm$ decays.

Figure 9 shows the visible energy histogram after removing events with particles of energy over 200 GeV entering the region .995< $|\cos(\theta)|$ <.99995.

[10]see Appendix A Figure 21.

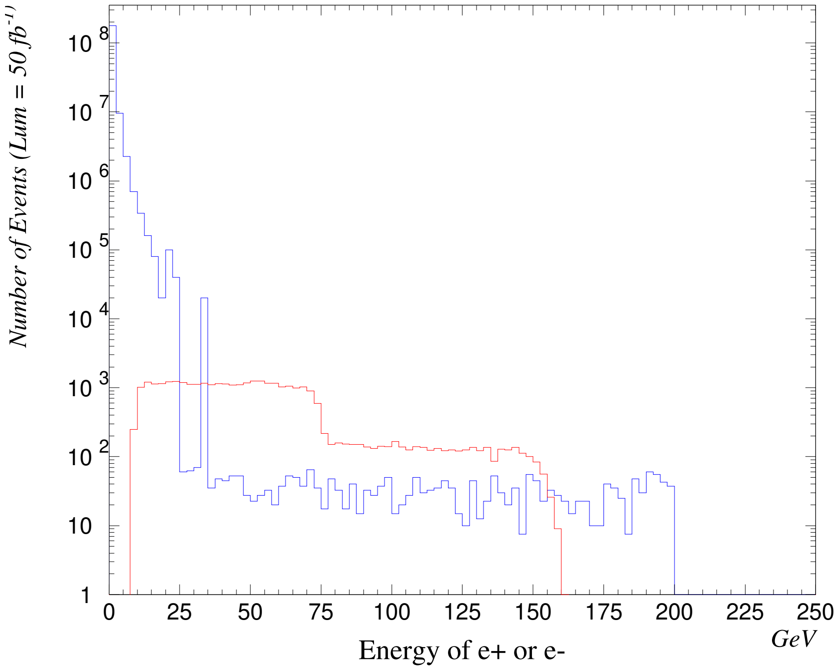

Figure 8: E_{e^+,e^-} for Supersymmetric signal (red) and Standard Model background (blue) following cut to limit events to those with energy in the forward direction less than 0.4 E_{cm}. E_{cm} = 500 GeV, 80% right polarization.

At this point, enough background events have been removed to increase the number of $\gamma^*\gamma^*$ events we generate. The histograms that follow are still 50 fb^{-1}, but there are now 6.9 x 10^6 $\gamma^*\gamma^*$ events, and each is scaled by 200 (instead of 20,000).

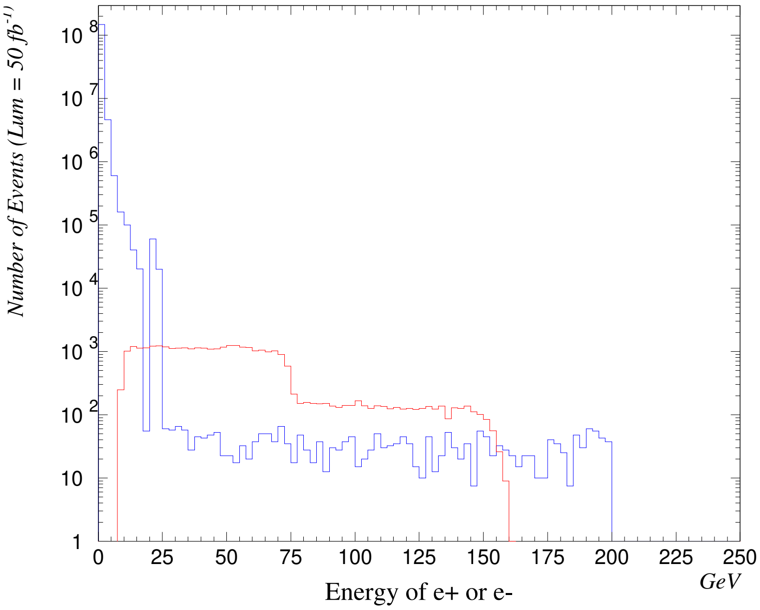

Figure 9: E_{e^+,e^-} for Supersymmetric signal (red) and Standard Model background (blue) following cut to limit events to those with no particles of energy greater than 200 GeV in .995$<|\cos(\theta)|<$.99995. E_{cm} = 500 GeV, 80% right polarization.

Cut 5 Initial state electrons and positrons often emit a γ^* and then escape undetected by traveling inside a smaller radius than the luminosity monitor. The angular distribution of these particles is shown in Figure 10. One can

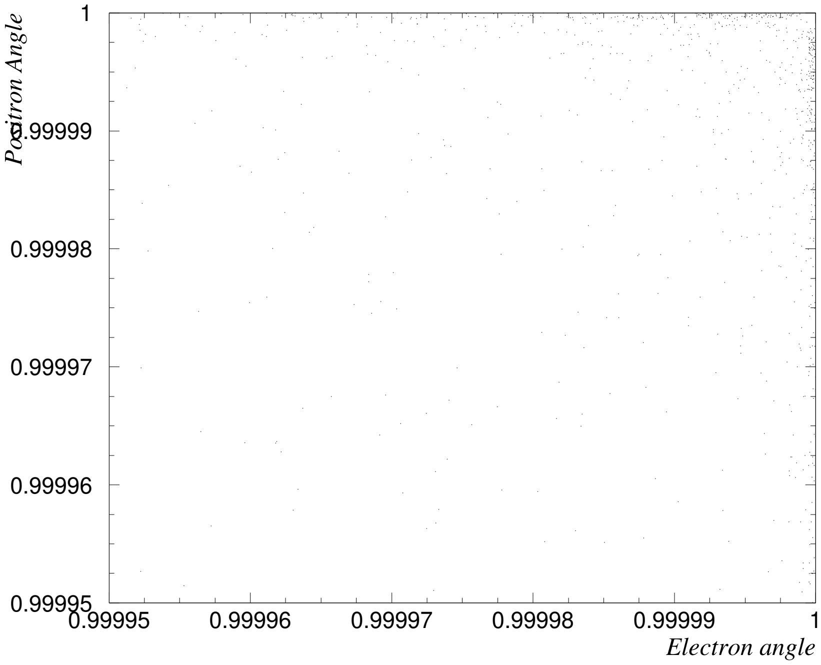

Figure 10: Angle of each charged particle for two photon $\rightarrow$ e^+e^- events inside of $|\text{coszeta}| = .99995$. Number of events is equivalent to 50 fb^{-1}.

see from Figure 10 that the angles of the particles most often tend to be very close to coszeta = 1.

In Figure 11 we plot the energy of the particles. The histogram on the right is a magnification of that on the left.

It is interesting to note that usually when an event has one particle with energy near 250 GeV, the other charged particle in the event has lower energy. We therefore remove events with two particles inside $|\text{coszeta}| = .99995$ when one of the particles has energy of less than 243 GeV.

At this time, we also adjust the cut on the luminosity monitor. We now remove events with more than 100 GeV entering the luminosity monitor. Figure 12 shows the energy histogram for events that remain after these cuts.

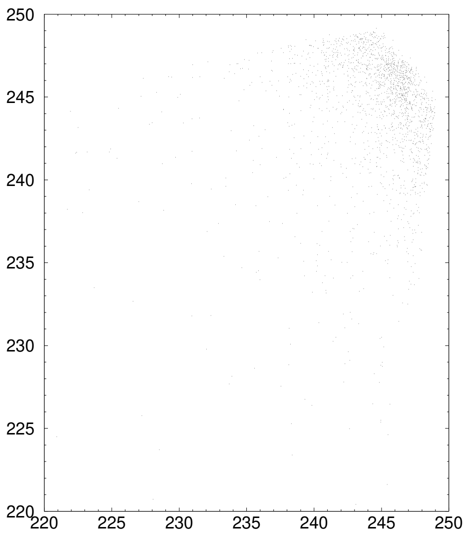

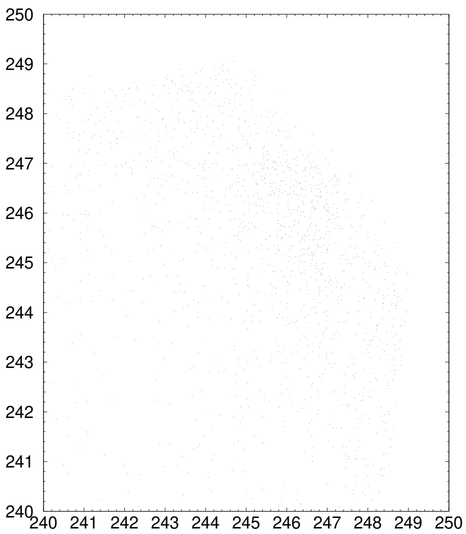

Figure 11: Energy of electrons vs. energy of positrons for two photon $\rightarrow$ e^+e^- events inside of $|\text{coszeta}| = .99995$. Number of events is equivalent to 50 fb^{-1}.

Cut 6 Figure 13 shows the angle between the electron and the positron for the Supersymmetric Signal and the Standard Model background after the cuts we have made so far.

We now make a cut to remove events with cos theta less than or equal to -0.96. The energy histograms that result are shown in Figure 14.

This cut removes events where the two visible particles are moving in opposite directions. These particles generally have very high energy and therefore this cut does not affect the low-energy endpoint of our Supersymmetric signal.

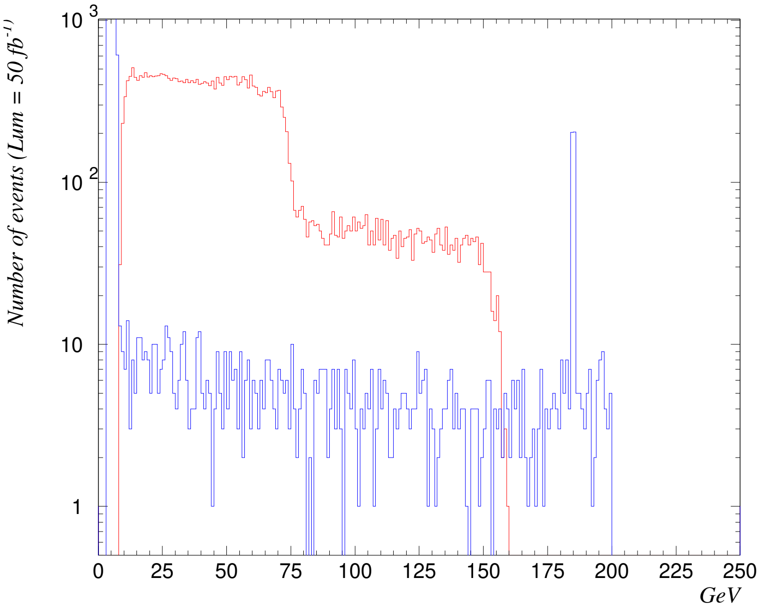

Figure 12: E_{e^+,e^-} for Supersymmetric signal (red) and Standard Model background (blue) following a cut to remove events with energy greater than 100 GeV in the luminosity monitor and following a cut to remove events with two particles inside |coszeta| = .99995 when one of the particles has energy of less than 243 GeV. E_{cm} = 500 GeV, 80% right polarization.

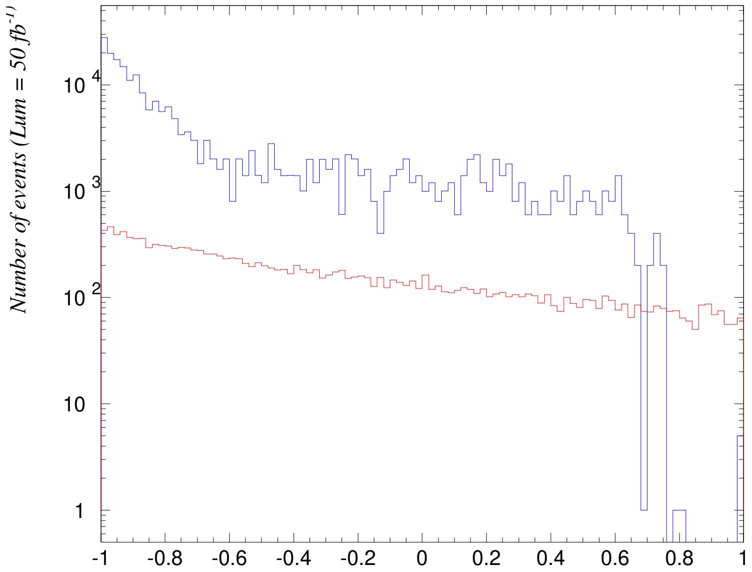

Figure 13: Angle between electron and positron for Supersymmetric signal (red) and Standard Model background (blue) following all cuts. E_{cm} = 500 GeV, 80% right polarization.

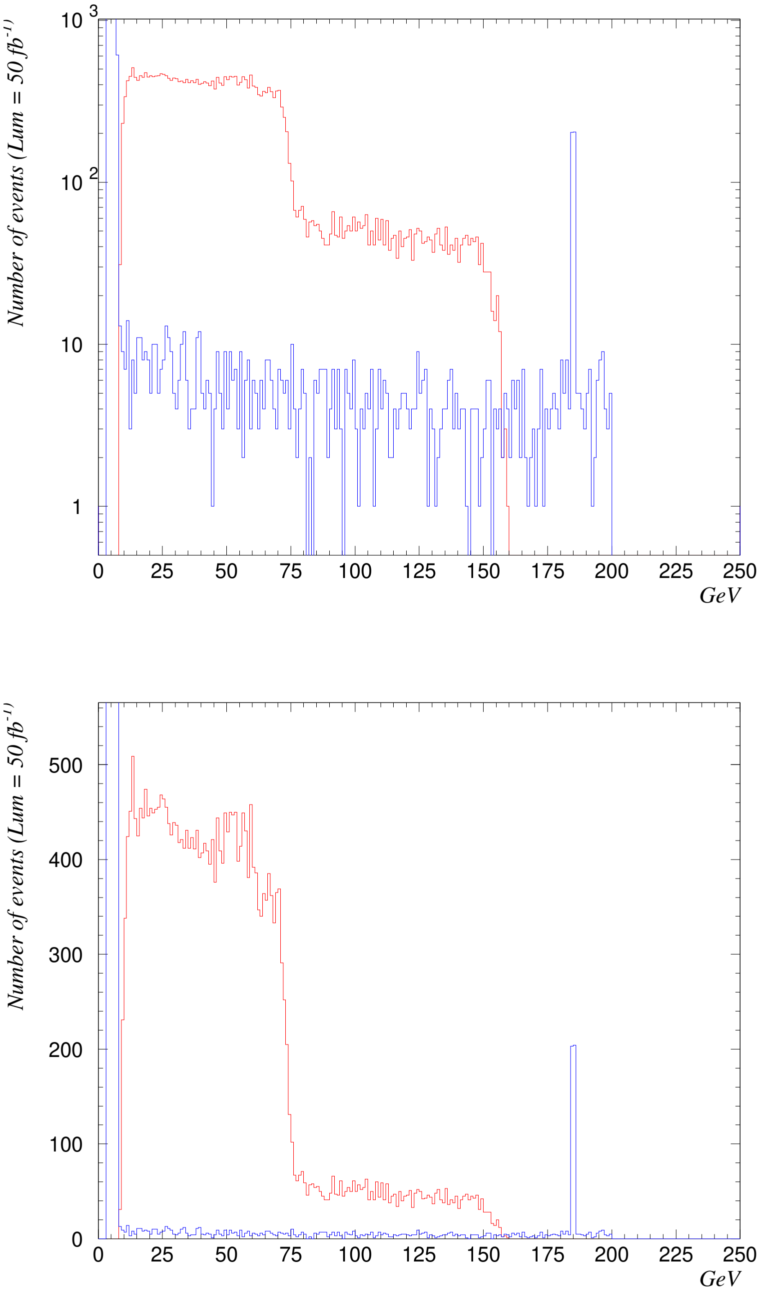

Figure 14: E_{e^+,e^-} for Supersymmetric signal (red) and Standard Model background (blue) following cut to remove events with the angle between the electron and positron less than or equal to -0.96. Top plot logarithmic, bottom plot linear. E_{cm} = 500 GeV, 80% right polarization.

This set of cuts is the most effective way we found of reducing the background without changing the endpoints of the visible energy histogram for the signal. To summarize, the cuts we used are:

- All events must have exactly two visible particles: one e^+ and one e^-.
- All events mush have less than 1 GeV visible energy between .90< $|\cos(\theta)|$ <.995.
- Limit events to those with energy in the forward direction less than 0.4 E_{cm}.
- Remove events that have particles with energy of over 200 GeV entering the region .995< $|\cos(\theta)|$ <.99995.
- Remove events with energy greater than 100 GeV in the luminosity monitor and remove events with two particles inside |coszeta| = .99995 when one of the particles has energy of less than 243 GeV.
- Remove events with the angle between the electron and positron less than or equal to -0.96.

When making these cuts, we were concerned with maintaining both the edges and the shape of the Supersymmetric signal. It is important to maintain the edges of the Supersymmetric signal because they correspond to the minimum and maximum energies of the event. These endpoints are used to calculate the masses of the Supersymmetric particles. It is important to maintain the shape of the signal because we apply a gaussian fit function to the E_{e^+,e^-} energy histogram. The endpoints of the gaussian change if the shape of the histogram changes, as will be shown in the next section.

Energy in the Backward Direction We initially planned to make a cut when the energy in the backward direction was zero. The backward direction is defined to be the hemisphere with less energy. This cut would remove background events when one Z^0 decays into two ν and one Z^0 decays into two leptons, or when both $W^\pm$ decay into $\ell\nu$. Depending on the momentum (both direction and velocity) of the Z^0 and the $W^\pm$, the visible particles may propagate in the forward direction and the invisible ν may propagate in the backward direction. In this case, the event would be cut. Unfortunately, this also cuts signal events where the two visible particles go in the forward direction, and the two invisible particles (the neutralinos) both go backward. After making this cut, we plot the energy histograms shown in Figure 15.

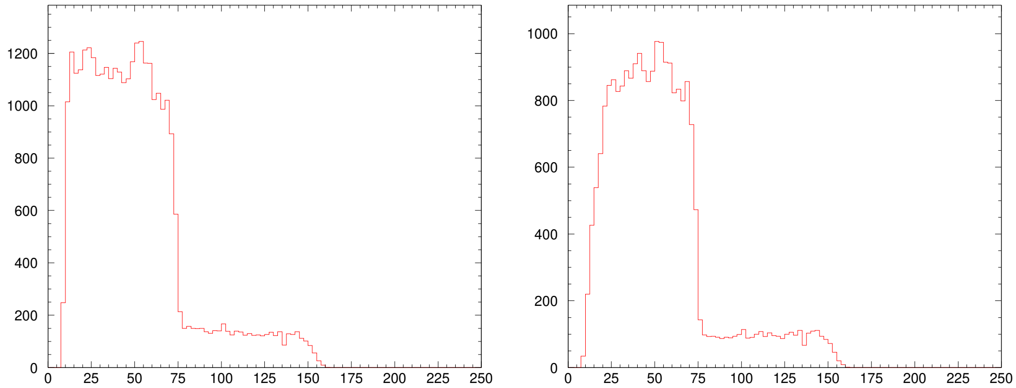

Figure 15: E_{e^+,e^-} for Supersymmetric signal (red) following cut to limit events to those with energy in the backward direction greater than zero. This cut is not used because it changes the shape of the energy histogram. Changing the shape by this much, even though the endpoints are maintained, causes the fit to the plot to have a value of E_{min} = 13.29 GeV, which is not acceptable.

6.1.2 500 GeV, 80% left polarization

We carried out the same analysis for 80% left-polarized incident electrons as we did for 80% right-polarized incident electrons. The effect of changing the polarization is that the cross section of the $\tilde{e}_R^{\pm}$ changes (as shown in Table 8), and the cross section of the W$^{\pm}$ changes (as shown in Table 3).

Because the angular distribution for left- and right-handed polarizations are the same, we were able to use the same cuts as we used previously to reduce the background and enhance the signal.

The resulting 80% left-polarized, 500 GeV plot for the combined $\tilde{e}_R^{\pm}\tilde{e}_R^{\mp}$, $\tilde{e}_R^{\pm}\tilde{e}_L^{\mp}$, $\tilde{e}_L^{\pm}\tilde{e}_L^{\mp}$ selectron production is shown in Figure 16.

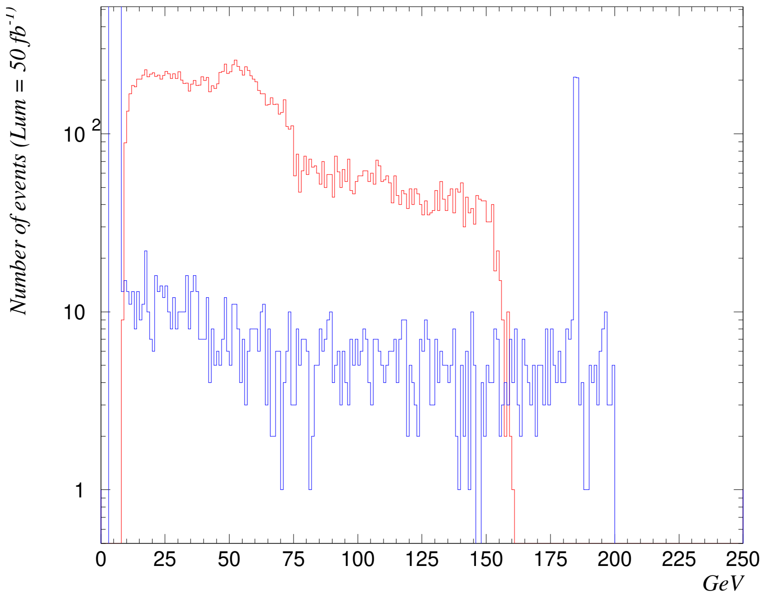

Figure 16: E$_{e^+,e^-}$ for Supersymmetric signal (red) and Standard Model background (blue) following all cuts. Cuts are exactly the same as those applied to the 80% right- polarized events. E$_{cm}$ = 500 GeV, 80% left polarization.

7 Mass Calculation

In 1983, at CERN in Switzerland, scientists collided protons and antiprotons to produce W bosons. Some of the W particles decayed into an electron and a neutrino. The neutrino escaped unnoticed, but the high energy electron was detected in the calorimeter. By measuring the energy of the electron, and using conservation laws to determining what the energy of the neutrino must have been, the scientists were able to infer the existence of the W boson and to determine its mass [3, p. 58]. We use a similar method to determine the masses of the Supersymmetric particles [4].[11]

Following all of the cuts, we can plot the energy of each electron and positron, and use their minimum and maximum energies to determine the masses of the Supersymmetric particles. Figure 17 shows the $E_{e^\pm}$ for the sum of $\tilde{e}_L^\pm \tilde{e}_L^\mp$, $\tilde{e}_R^\pm \tilde{e}_L^\mp$, and $\tilde{e}_R^\pm \tilde{e}_R^\pm$ (shown as a red line), and the Standard Model background (shown in blue).

Figure 18 shows the energy distributions of the Supersymmetric signals we are trying to see. This figure shows the energy of each of the electrons and positrons remaining in the *signal only* following the cuts we applied to remove the background and enhance the signal. The purpose of this figure is to show what the Supersymmetric signals that we are trying to see look like, *even though this is not information that can be had from the actual detector.* We need to determine the endpoints of the combination of the Supersymmetric signal and the Standard Model background shown in Figure 17.

These endpoints are used to calculate the masses of the Supersymmetric particles.

The masses of all right-handed leptons are the same, and the masses of all left-handed leptons are the same, but the masses of the left-handed leptons are different from the masses of the right-handed leptons. Therefore, we need to determine both the right-handed lepton mass and the left-handed lepton mass. As shown in Table 8, when we change the polarization from 80% right to 80% left, the cross section changes most visibly for the right selectron (from 280 fb^{-1} to 85 fb^{-1}), so the part of the histogram that changes the most with the different polarizations is the $\tilde{e}_R\tilde{e}_R$ signal. In Figure 17, the part of the graph between about 10 and 75 GeV changes the most, so those events are the $\tilde{e}_R\tilde{e}_R$ signal.

[11] The mathmatical method for determining the masses of the Supersymmetric particles using the energy of the electron is discussed in Appendices B and C.

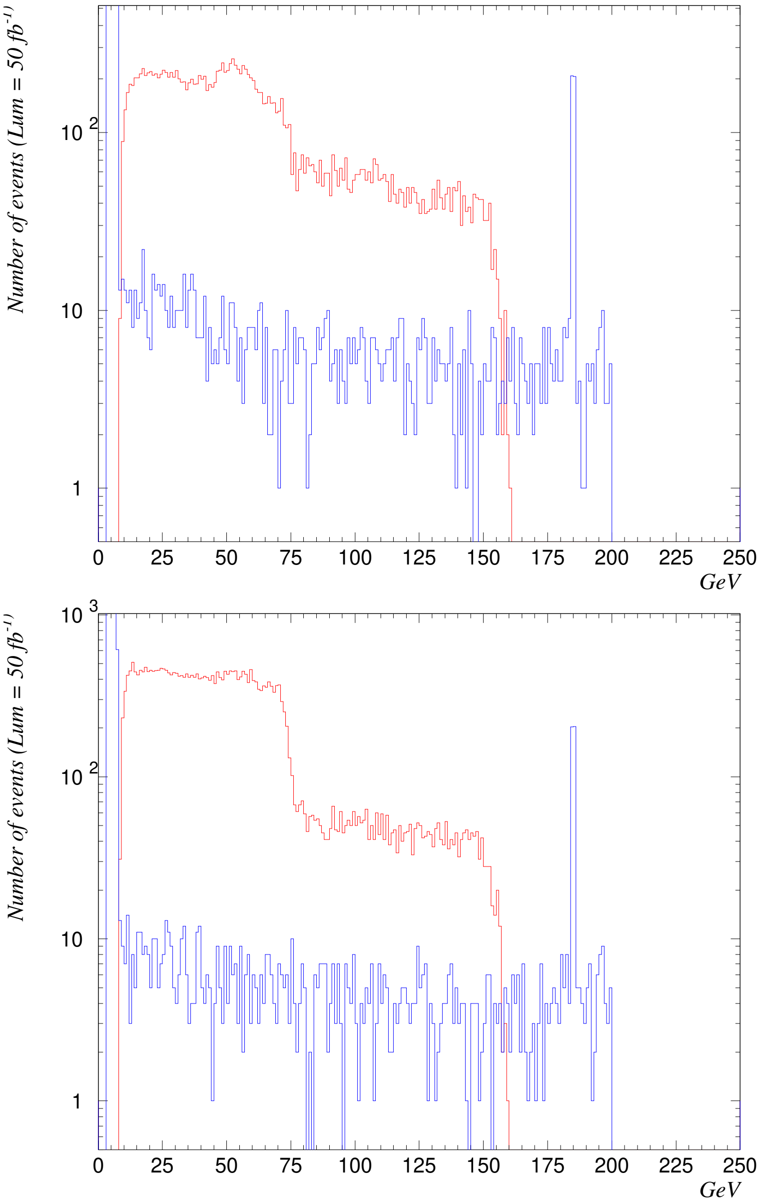

Figure 17: $E_{e^\pm}$ for Supersymmetric signal and Standard Model background following cuts to reduce background. Top plot is 80% left polarization, bottom plot is 80% right polarization. E_{cm} = 500 GeV.

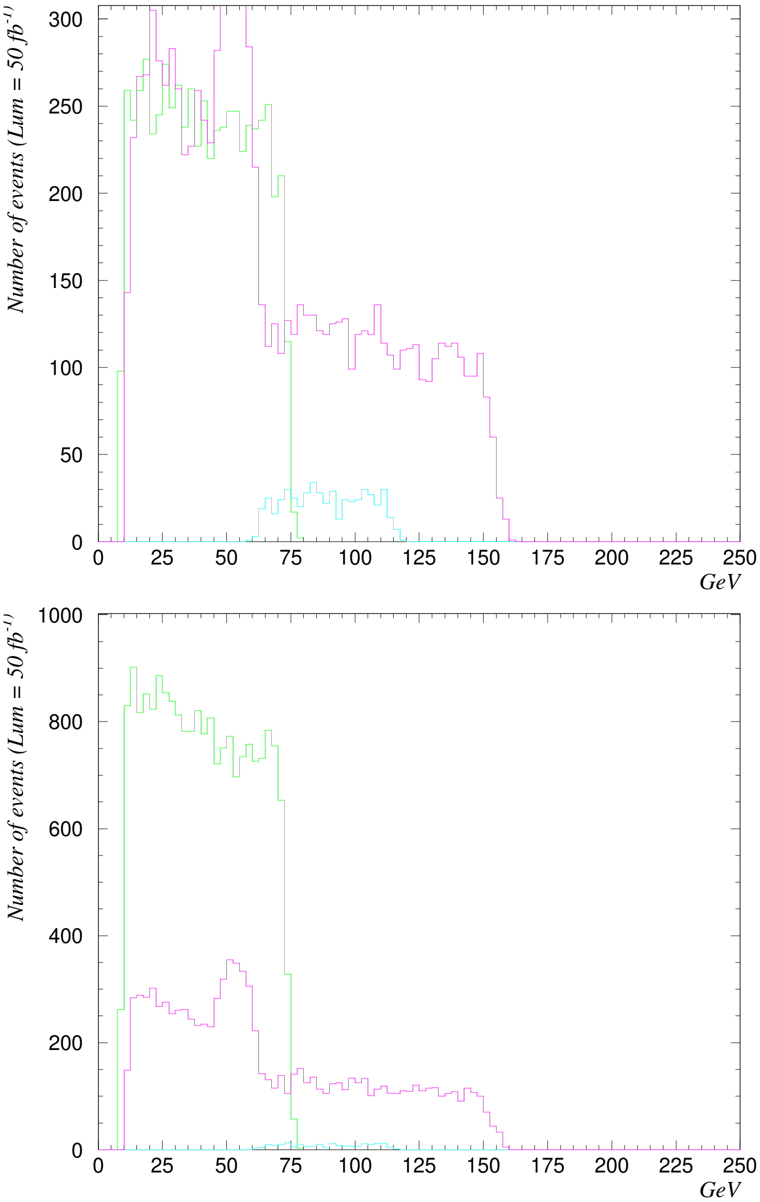

Figure 18: $E_{e^\pm}$ for Supersymmetric signal ($\tilde{e}_L^\pm \tilde{e}_L^\mp$ blue, $\tilde{e}_R^\pm \tilde{e}_R^\mp$ green, $\tilde{e}_R^\pm \tilde{e}_L^\mp$ fuchsia) following cuts to remove background events. E_{cm} = 500 GeV; top plot is 80% left polarization, bottom plot is 80% right polarization.

Figure 19 shows the sum of the Supersymmetric signal and background shown in Figure 17, with a box function convoluted with a gaussian fit to the part of the histogram that changes the most with polarization.

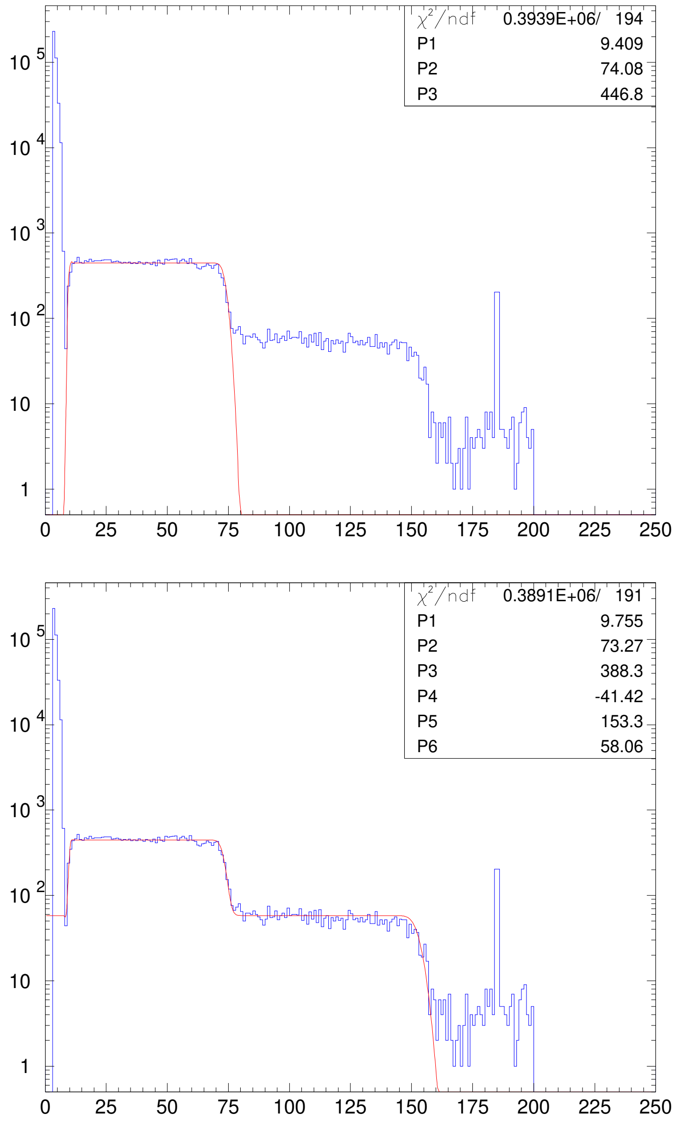

Figure 19: Fit functions convoluted to fit $E_{e^\pm}$ for Supersymmetric signal after performing cuts to isolate signal from Standard Model background. Top plot: Box function convoluted with a gaussian applied to determine endpoints of $\tilde{e}^{\pm}_R\tilde{e}^{\mp}_R$. Bottom plot: Two boxes convoluted with gaussians applied to determine E_{max} of complete electron-positron sample. 500 GeV, 80% right polarization.

We use the endpoints of the box fit to the $\tilde{e}_R^{\pm}\tilde{e}_R^{\mp}$ signal as the values of E_{min} and E_{max}. In Figure 19, top, in the box in the upper right hand corner, P1 is the left endpoint (E_{min} = 9.40 GeV), P2 is the right endpoint (E_{max} = 74.08 GeV), and P3 is the height of the box. We use these values in the following equations, where s is E_{cm}^2:

$$\begin{aligned} m_A^2 &= E_{cm}^2 \left[\frac{E_{Dmax}E_{Dmin}}{(E_{Dmax}+E_{Dmin})^2} \right] \\ m_C^2 &= E_{cm}^2 \left[\frac{E_{Dmax}E_{Dmin}}{(E_{Dmax}+E_{Dmin})^2} \right] - 2E_{cm}\frac{E_{Dmax}E_{Dmin}}{E_{Dmax}+E_{Dmin}} \end{aligned}$$

Once we know the masses of the $\tilde{\ell}_R$ and the $\tilde{\chi}_1^0$, we use them with E_{max} from the histogram of the energy of all electrons and positrons (Figure 19, bottom) to find the mass of the $\tilde{\ell}_L$. The mass of the $\tilde{\ell}_L$ is given by

$$\begin{aligned} m_B^4 & \ (E_{cm} - 2E_{Dmax}) + \\ m_B^2 & \ (4E_{cm}E_{Dmax}^2 - 2E_{cm}^2E_{Dmax} + 2m_A^2E_{Dmax} + 2m_C^2E_{Dmax} - 2E_{cm}m_C^2) + \\ & \ 2m_C^2E_{cm}^2E_{Dmax} - 2m_A^2m_C^2E_{Dmax} + E_{cm}m_C^4 = 0 \end{aligned}$$

where E_{max} = 153.3 GeV.

Table 9 shows the masses of the $\tilde{\chi}_1^0$, the $\tilde{\ell}_R$, and the $\tilde{\ell}_L$.

Table 9: Masses of Supersymmetric particles (in GeV) calculated using endpoint energies.

Particle	Known Mass	Calculated Mass	Discrepancy
$\tilde{\chi}_1^0$	128.702	128.993	0.23%
$\tilde{\ell}_R$	156.952	158.053	0.70%
$\tilde{\ell}_L$	238.213	239.427	0.51%

8 Conclusion

We have simulated the expected number of electron-positron events at a luminosity of 50 fb^{-1} per year and we have isolated the signal from Supersymmetric selectrons using cuts that are reproduceable in a particle detector. By noticing that the cross section of right-handed selectrons changes as a function of polarization, we have isolated the signal of right-handed selectrons. We applied a fitting function to the isolated signal of right-handed electrons and right-handed positrons, and used the endpoints of the fit to determine the masses of the $\widetilde{\ell}_R$ and the $\widetilde{\chi}_1^0$. We then used these masses and the endpoints of the histogram of my whole sample of electrons and positrons to find the mass of the $\widetilde{\ell}_L$. The masses we have obtained are in good agreement with the theoretically derived values.

The endpoints of the signal are virtually unchanged, which is important in the calculation of the masses, since the endpoints correspond to the minimum and maximum energies of the $e^{\pm}$.

These results are promising. The cuts are reproduceable by an actual detector, and the results can be used to help determine the parameters used in the construction of the next linear accelerator.

9 Appendix A: The New Linear Collider

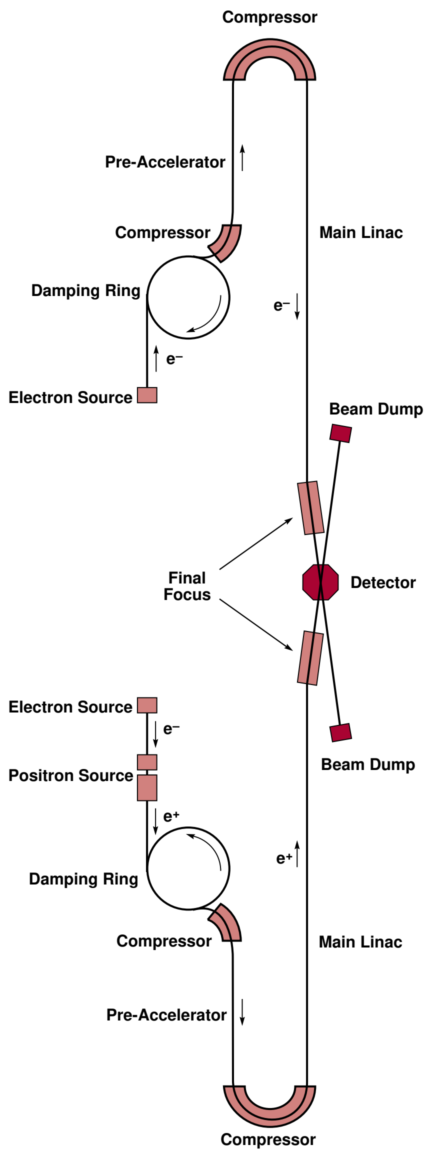

Figure 20: The proposed New Linear Collider

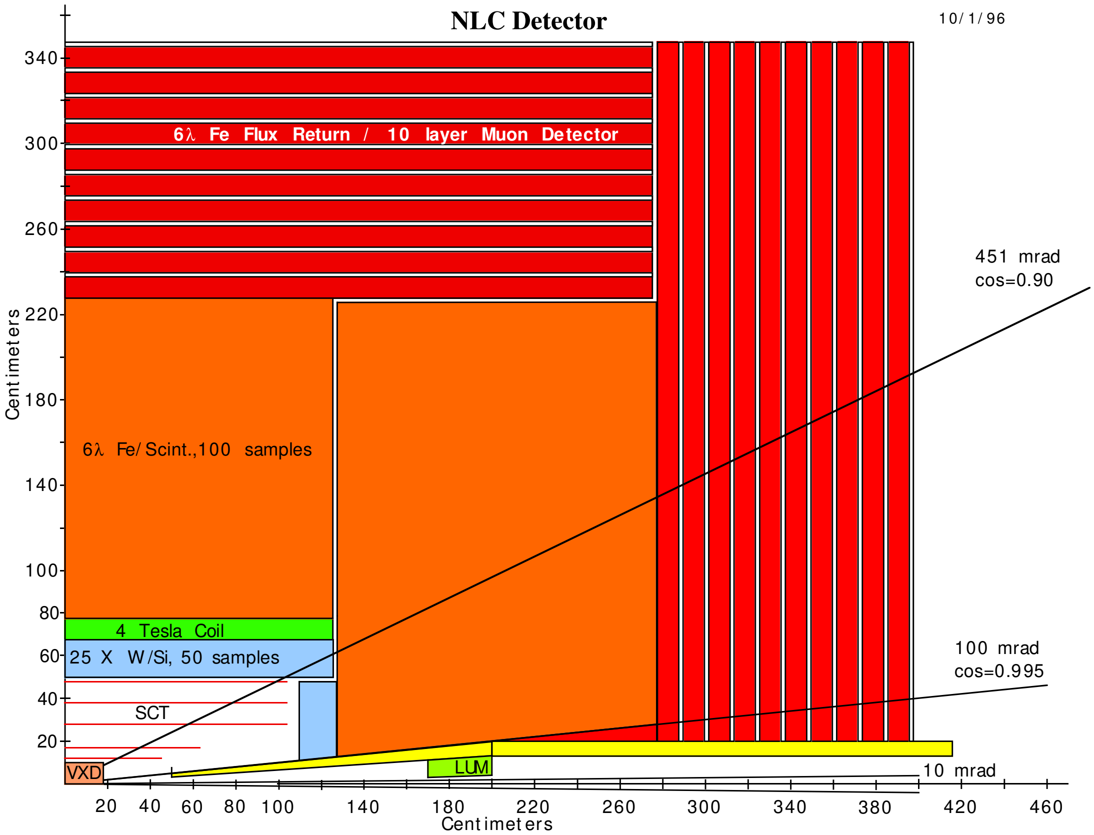

Figure 21: The proposed New Linear Collider's Detector

10 Appendix B: Method for Determining the Mass of the Right Selectron and the Mass of the Neutralino

In a reaction involving $e^+ + e^- \to A + B$, where A and B have the same mass[12], we can determine the masses of A and C by examining the endpoints of the energy spectrum of D: E_{Dmin} and E_{Dmax}. In the Feynman diagram below,

[12]the case where A and B have different masses is treated in Appendix B

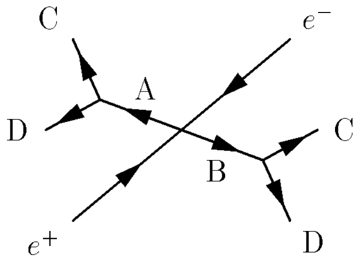

$$\begin{aligned} A &= \tilde{e}_R^+ \\ B &= \tilde{e}_R^- \\ C &= \tilde{\chi}_1^0 \\ D &= e^\pm \end{aligned}$$

We shall use the following notation throughout this section:

$$\begin{aligned} p_A &= \text{momentum of A} \\ m_A &= \text{mass of A} \\ E_A &= \text{energy of A} \end{aligned}$$

We set c = 1 and disregard it.

Relativity

$$E_D^{lab} = \gamma(E_D^{cm} + \beta p_D^{cm} cos(\theta))$$

By varying θ, we can find E_{Dmin}^{lab} and E_{Dmax}^{lab}. Since D is an electron its mass can be neglected; $E_D^{cm} = p_D^{cm}$

$$E_{Dmax}^{lab} = \gamma(1+\beta)E_D^{cm} \tag{1}$$
$$E_{Dmin}^{lab} = \gamma(1-\beta)E_D^{cm} \tag{2}$$

We need an expression for β, γ, and E_D^{cm}.

Expression for E_D^{cm} In the center of mass frame of A,

$$\begin{aligned} E_A &= m_A \\ E_A &= E_D + E_C \end{aligned}$$

$$
\begin{aligned}
m_A &= E_D + E_C \\
E_C &= m_A - E_D \\
E_C^2 &= m_A^2 - 2E_D m_A + E_D^2 \\
p_C^2 + m_C^2 &= m_A^2 - 2E_D m_A + p_D^2 + m_D^2
\end{aligned}
$$

because $p_C^2 = p_D^2$,

$$
m_C^2 = m_A^2 - 2E_D m_A + m_D^2
$$

if we neglect m_D,

$$
E_D^{cm} = \frac{m_A^2 - m_C^2}{2m_A}
$$

$$
E_D^{cm} = \frac{m_A}{2}\left(1 - \frac{m_C^2}{m_A^2}\right) \tag{3}
$$

Expression for β

$$
\begin{aligned}
\beta &= \frac{p_A}{E_A} \\
&= \sqrt{1 - \frac{m_A^2}{E_A^2}} \\
E_{cm}^2 &= 4E_A^2
\end{aligned}
$$

$$
\beta = \sqrt{1 - \frac{4m_A^2}{E_{cm}^2}} \tag{4}
$$

Expression for γ

$$
\begin{aligned}
\gamma &= \frac{1}{\sqrt{1-\beta^2}} \\
\sqrt{1-\beta^2} &= \sqrt{\frac{4m_A^2}{E_{cm}^2}}
\end{aligned}
$$

$$
\gamma = \frac{E_{cm}}{2m_A} \tag{5}
$$

Plugging In If we plug (3), (4), and (5) into equations (1) and (2) we get

$$
\begin{aligned}
E_{Dmax} &= \frac{E_{cm}}{2m_A}\left(1+\sqrt{1-\frac{4m_A^2}{E_{cm}^2}}\right)\frac{m_A}{2}\left(1-\frac{m_C^2}{m_A^2}\right) \\
&= \frac{E_{cm}}{4}\left(1+\sqrt{1-\frac{4m_A^2}{E_{cm}^2}}\right)\left(1-\frac{m_C^2}{m_A^2}\right)
\end{aligned}
$$

$$
E_{Dmin} = \frac{E_{cm}}{4}\left(1-\sqrt{1-\frac{4m_A^2}{E_{cm}^2}}\right)\left(1-\frac{m_C^2}{m_A^2}\right)
$$

Algebra Now we have two equations and two unknowns. We solve for m_A and m_C

$$
\begin{aligned}
\frac{E_{Dmax}}{E_{Dmin}} &= \frac{\left(1+\sqrt{1-\frac{4m_A^2}{E_{cm}^2}}\right)}{\left(1-\sqrt{1-\frac{4m_A^2}{E_{cm}^2}}\right)} \\
E_{Dmax}\left(1-\sqrt{1-\frac{4m_A^2}{E_{cm}^2}}\right) &= E_{Dmin}\left(1+\sqrt{1-\frac{4m_A^2}{E_{cm}^2}}\right) \\
\frac{E_{Dmax}-E_{Dmin}}{E_{Dmax}+E_{Dmin}} &= \sqrt{1-\frac{4m_A^2}{E_{cm}^2}} \\
&= \beta
\end{aligned}
$$

$$
\begin{aligned}
\beta &= \frac{E_{Dmax}-E_{Dmin}}{E_{Dmax}+E_{Dmin}} \\
1-\beta &= \frac{2E_{Dmin}}{E_{Dmax}+E_{Dmin}} \\
1+\beta &= \frac{2E_{Dmax}}{E_{Dmax}+E_{Dmin}}
\end{aligned}
$$

An Expression for m_A^2 When we developed an equation for γ, we found that

$$
\begin{aligned}
1-\beta^2 &= \frac{4m_A^2}{E_{cm}^2} \\
\frac{4m_A^2}{E_{cm}^2} &= (1+\beta)(1-\beta) \\
m_A^2 &= \frac{E_{cm}^2(1+\beta)(1-\beta)}{4}
\end{aligned}
$$

$$
m_A^2 = E_{cm}^2\left[\frac{E_{Dmax}E_{Dmin}}{(E_{Dmax}+E_{Dmin})^2}\right] \tag{6}
$$

An Expression for m_C^2 Recalling the equation we had for E_{Dmin}:

$$
\begin{aligned}
E_{Dmin} &= \frac{E_{cm}}{4}(1-\beta)\left(1-\frac{m_C^2}{m_A^2}\right) \\
E_{Dmin} &= \frac{E_{cm}}{4}\frac{2E_{Dmin}}{E_{Dmax}+E_{Dmin}}\left(1-\frac{m_C^2}{m_A^2}\right)
\end{aligned}
$$

We can divide by E_{Dmin} since it is non-zero.

$$
\begin{aligned}
1 &= \frac{E_{cm}}{2(E_{Dmax}+E_{Dmin})}\left(1-\frac{m_C^2}{m_A^2}\right) \\
\frac{2(E_{Dmax}+E_{Dmin})}{E_{cm}} &= \left(1-\frac{m_C^2}{m_A^2}\right) \\
\frac{m_C^2}{m_A^2} &= 1-\frac{2(E_{Dmax}+E_{Dmin})}{E_{cm}}
\end{aligned}
$$

$$
m_C^2 = \left[1-\frac{2(E_{Dmax}+E_{Dmin})}{E_{cm}}\right]m_A^2 \tag{7}
$$

We can either calculate m_A and plug that in, or plug m_A^2 directly into m_C^2 and get

$$
m_C^2 = E_{cm}^2\left[\frac{E_{Dmax}E_{Dmin}}{(E_{Dmax}+E_{Dmin})^2}\right]-2E_{cm}\frac{E_{Dmax}E_{Dmin}}{E_{Dmax}+E_{Dmin}} \tag{8}
$$

11 Appendix C: Method for Determining the Mass of the Left Selectron

The following two-body-decay mass determination is used to find the mass of the left selectron in cases where $e^+ + e^- \rightarrow \tilde{e}_L + \tilde{e}_R$. This case is more difficult than that in Appendix A because the mass of the $\tilde{e}_L$ is different than that of the mass of the $\tilde{e}_R$, and within the energy histogram of the $\tilde{e}_L\tilde{e}_R$, there are edges that cannot be seen, as shown in Figure 18. It is necessary to develop a method for calculating the mass of the $\tilde{e}_L$ using only Emax and the already known masses of the $\tilde{e}_R$ and $\tilde{\chi}_1^0$.

In the following reaction we can determine the mass of B if we know the maximum energy of particle D and the mass of particles A and C. In the two-body decay Feynman diagram shown in Appendix B,

$$\begin{aligned} A &= \tilde{e}_R^{\mp} \\ B &= \tilde{e}_L^{\pm} \\ C &= \tilde{\chi}_1^0 \\ D &= e^{\pm} \end{aligned}$$

where A and B have different masses.

We will use the following notation throughout this section:

$$\begin{aligned} p_A &= \text{momentum of A} \\ m_A &= \text{mass of A} \\ E_A &= \text{energy of A} \end{aligned}$$

$$c = \text{speed of light, which we disregard as a constant.}$$

Relativity We know from relativity that

$$E_D^{lab} = \gamma(E_D^{cm} + \beta p_D^{cm}\cos\theta)$$

where E_D^{cm} is the energy of D (the electron) in the center of mass frame of B. By varying θ, we can determine E_{Dmax}^{lab}.

$$E_{Dmax}^{lab} = \gamma(E_D^{cm} + \beta p_D^{cm}).$$

We drop the "lab" subscript. Since D is an electron, its mass is negligible compared to the other particles we are working with. Therefore, $E_D = p_D$.

$$E_{Dmax} = \gamma E_D^{cm}(1+\beta)$$

Since we are looking for a relation involving E_{Dmax} we are on the right track. We need to determine expressions for γ, β, and E_D^{cm}.

An Equation for β

$$\begin{aligned} \beta &= \frac{p_B}{E_B} \\ p_B &= \sqrt{E_B^2 - m_B^2} \\ \beta &= \sqrt{1 - \frac{m_B^2}{E_B^2}} \end{aligned}$$

An Equation for γ

$$\begin{aligned} \gamma &= \frac{1}{\sqrt{1-\beta^2}} \\ &= \frac{E_B}{m_B} \end{aligned}$$

An Equation for E_D^{cm} In the center of mass of B,

$$\begin{aligned} E_B &= m_B = E_D + E_C \\ E_D^{cm} &= m_B - E_C^{cm} \end{aligned}$$

Plugging In

$$E_{Dmax} = \frac{E_B}{m_B}\left(m_B - E_c^{cm}\right)\left(1 + \sqrt{1 - \frac{m_B^2}{E_B^2}}\right)$$

Now we need expressions for E_C^{cm} and for E_B.

Expression for E_C^{cm}

$$
\begin{aligned}
E_B &= E_C + E_D \\
E_D &= E_B - E_C \\
E_D^2 &= E_B^2 - 2E_BE_C + E_C^2 \\
p_D^2 + m_D^2 &= E_B^2 - 2E_BE_C + p_C^2 + m_C^2 \\
|p_C| &= |p_D| \\
m_D^2 &= E_B^2 - 2E_BE_C + m_C^2 \\
E_C^{cm} &= \frac{E_B^2 + m_C^2 - m_D^2}{2E_B}
\end{aligned}
$$

Since m_D is the mass of the electron, which is small compared to the other masses, we can neglect it. Since we are in the center of mass frame of particle B, $E_B = m_B$.

$$
E_C^{cm} = \frac{m_B^2 + m_C^2}{2m_B}
$$

Expression for E_B In a method similar to that for finding E_C^{cm}, we find that

$$
E_B = \frac{E_{cm}^2 + m_B^2 - m_A^2}{2E_{cm}}
$$

Plugging In

$$
E_{Dmax} = \frac{E_{cm}^2 + m_B^2 - m_A^2}{2E_{cm}m_B}\left(m_B - \frac{m_B^2 + m_C^2}{2m_B}\right)\left(1 + \sqrt{1 - \frac{4m_B^2E_{cm}^2}{(E_{cm}^2 + m_B^2 - m_A^2)^2}}\right)
$$

Algebra

$$
\begin{aligned}
E_{Dmax} &= \frac{(E_{cm}^2 + m_B^2 - m_A^2)(m_B^2 - m_C^2)}{4m_B^2E_{cm}}\left[1 + \sqrt{\frac{(E_{cm}^2 + m_B^2 - m_A^2)^2 - 4m_B^2E_{cm}^2}{(E_{cm}^2 + m_B^2 - m_A^2)^2}}\right] \\
E_{Dmax} &= \frac{(E_{cm}^2 + m_B^2 - m_A^2)(m_B^2 - m_C^2)}{4m_B^2E_{cm}}\left[1 + \frac{\sqrt{(E_{cm}^2 - m_B^2 - m_A^2)^2 - 4m_B^2m_A^2}}{E_{cm}^2 + m_B^2 - m_A^2}\right]
\end{aligned}
$$

$$\frac{4m_B^2 E_{cm} E_{Dmax}}{m_B^2 - m_C^2} = (E_{cm}^2 + m_B^2 - m_A^2) + \sqrt{(E_{cm}^2 - m_B^2 - m_A^2)^2 - 4m_B^2 m_A^2}$$

$$\left[\frac{4m_B^2 E_{cm} E_{Dmax}}{m_B^2 - m_C^2} - (E_{cm}^2 + m_B^2 - m_A^2)\right]^2 = (E_{cm}^2 - m_B^2 - m_A^2)^2 - 4m_B^2 m_A^2$$

Squaring the left-hand side, we get

$$\frac{16m_B^4 E_{cm}^2 E_{Dmax}^2}{(m_B^2 - m_C^2)^2} - \frac{(8m_B^2 E_{cm} E_{Dmax})(E_{cm}^2 + m_B^2 - m_A^2)}{m_B^2 - m_C^2} + (E_{cm}^2 + m_B^2 - m_A^2)^2$$

$$= (E_{cm}^2 - m_B^2 - m_A^2)^2 - 4m_B^2 m_A^2$$

$$\frac{16m_B^4 E_{cm}^2 E_{Dmax}^2}{(m_B^2 - m_C^2)^2} - \frac{(8m_B^2 E_{cm} E_{Dmax})(E_{cm}^2 + m_B^2 - m_A^2)}{m_B^2 - m_C^2}$$

$$+ E_{cm}^4 + 2E_{cm}^2 m_B^2 + m_B^4 - 2E_{cm}^2 m_A^2 - 2m_B^2 m_A^2 + m_A^4$$

$$= E_{cm}^4 - 2E_{cm}^2 m_B^2 + m_B^4 - 2m_A^2 E_{cm}^2 + 2m_B^2 m_A^2 + m_A^4 - 4m_B^2 m_A^2$$

A lot of things cancel, and since the mass of the left selectron is non-zero we can divide by m_B^2, leaving

$$\frac{4m_B^2 E_{cm} E_{Dmax}^2}{(m_B^2 - m_C^2)^2} - \frac{(2E_{Dmax})(E_{cm}^2 + m_B^2 - m_A^2)}{m_B^2 - m_C^2} + E_{cm} = 0$$

We multiply through by $(m_B^2 - m_C^2)^2$ and collect powers of m_B:

$$\begin{aligned}
m_B^4 \quad & (E_{cm} - 2E_{Dmax}) + \\
m_B^2 \quad & (4E_{cm} E_{Dmax}^2 - 2E_{cm}^2 E_{Dmax} + 2m_A^2 E_{Dmax} + 2m_C^2 E_{Dmax} - 2E_{cm} m_C^2) + \\
& 2m_C^2 E_{cm}^2 E_{Dmax} - 2m_A^2 m_C^2 E_{Dmax} + E_{cm} m_C^4 = 0
\end{aligned}$$

This equation is of the form $\mathrm{ax}^2 + \mathrm{bx} + \mathrm{c} = 0$, and can be solved using the quadratic equation (and a computer). Since the equation involves m_B^4 there are four roots. The two negative roots are disregarded because negative mass is not possible. The two positive roots are evaluated and one of them is disregarded using conservation of energy.

12 Appendix D: The relation between E_{cm} and E_{Dmin}

Because of possible design constraints on the NLD, it may be impossible to detect particles that enter the beamline at values of cos θ greater than .99995. In this case, it will be more difficult to remove $\gamma^*\gamma^*$ events with very low energy visible electrons or positrons. This will make it impossible to discern the low energy endpoint of the selectron's electron energy distribution. Nevertheless, since the lower energy endpoint is a function of the center of mass energy,[13]

$$E_{Dmin} \quad = \quad \frac{E_{cm}}{4}\left(1 - \sqrt{1 - \frac{4m_A^2}{E_{cm}^2}}\right)\left(1 - \frac{m_C^2}{m_A^2}\right)$$

one can adjust the lower energy endpoint by changing the center of mass energy.

If one plugs in fixed values for the masses of the $\tilde{e}_R$ and the $\tilde{\chi}_1^0$, plugs in various values for E_{cm}, and plots the values, Figure 22 results. This figure shows that at 500 GeV, the value for the minimum energy of the electron is about 9 GeV.

The threshold energy is the minimum center of mass energy needed to generate the particles in our production. Our threshold energy is 313.9; at that energy the lower energy endpoint is 25.59.

Interestingly, at a center of mass energy of 500 GeV, when the theoretically determined masses are plugged in, the value of the lower endpoint is 9.07. The value we ascertained using our fit function applied to the energy distribution after the cuts is 9.40.

[13]See Appendix B Equation (6).

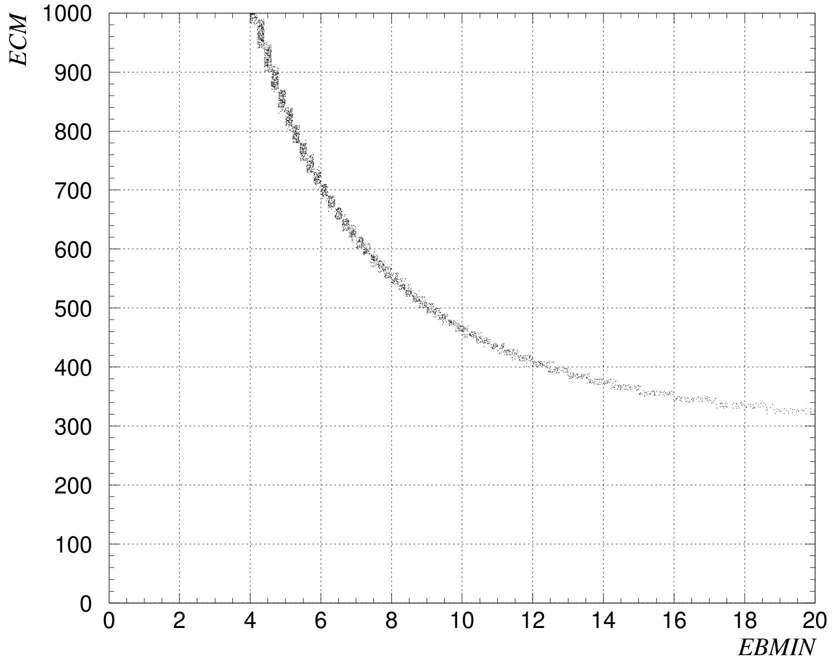

Figure 22: The relation between E_{cm} and E_{min}

References

[1] Haber, Howard and Kane, Gordon, "The Search for Supersymmetry; Probing Physics Beyond the Standard Model," *Physics Reports* 110 (1984).

[2] Langacker, Paul and Polonsky, Nir, "Uncertainties in Coupling Constant Unification," *Physical Review D* 47.9 (1 May 1993): 4028-4045.

[3] Haber, Howard and Kane, Gordon, "Is Nature Supersymmetric," *Scientific American* 254 (June, 1986): 52-60.

[4] Tsukamoto, Toshifumi, *et al.*, "Precision Study of Supersymmetry at Future Linear e^+ e^- Colliders," *Physical Review D* 51.7 (1 April 1995): 3153-3171.

[5] F. Paige, S. Protopopescu, in *Supercollider Physics*, p. 41, edited by D. Soper (World Scientific, 1986); H. Baer, F. Paige, S. Protopopescu, and X. Tata in *Proceedings of the Workshop on Physics at Current Accelerators and Supercolliders*, edited by J. Hewett, A. White, and D. Zeppenfeld, (Argonne National Laboratory, 1993).

[6] T. Sjöstrand, *Comp. Phys. Comm.* **82**, 74 (1994). S. Mrenna, *Simulating Supersymmetry with PYTHIA*, ANL-HEP-PR-96-63.

[7] G. Marchesini, B.R. Webber, G. Abbiendi, I.G. Knowles, M.H. Seymour and L. Stanco, Computer Phys. Commun. 67 (1992) 465.

[8] René Brun, Olivier Couet, Carlo Vandoni, Pietro Zanarini, edited by Michel Goossens, Version 1.07, October 1989, CERN, Geneva, Switzerland.

Bibliography

- Fayet, P., "Introduction to Supersymmetric and Grand-Unified Theories," invited talk at Rencontres du Vietnam, Hanoi, December 1993.
- Haber, Howard and Kane, Gordon, "The Search for Supersymmetry; Probing Physics Beyond the Standard Model," *Physics Reports* 110 (1984).
- Haber, Howard and Kane, Gordon, "Is Nature Supersymmetric," *Scientific American* 254 (June, 1986): 52-60.
- Kuhlman, S. *et al.*, *Physics and Technology of the Next Linear Collider*, BNL 52-502, Fermilab-PUB-96-112, LBNL-PUB-5425, SLAC Report 485, UCRL-ID-124160, submitted to the Snowmass '96 conference, June 1996.
- Langacker, Paul and Polonsky, Nir, "Uncertainties in Coupling Constant Unification," *Physical Review D* 47.9 (1 May 1993): 4028-4045.
- Peskin, Michael E., "The Experimental Investigation of Supersymmetric Breaking," preprint of the proceedings of the Yukawa International Seminar, Kyoto, Japan, August 21-25, 1995; Stanford Linear Accelerator Center Publication 7133, April 1996.
- Tsukamoto, Toshifumi, *et al.*, "Precision Study of Supersymmetry at Future Linear $e^+ e^-$ Colliders," *Physical Review D* 51.7 (1 April 1995): 3153-3171.